INDC(JPN)-165/U

JAERI-M
93-124

MEASUREMENT OF FORMATION CROSS SECTIONS OF SHORT-LIVED NUCLEI BY 14 MeV NEUTRONS

——Ru, Pd, Cd, Sn——

June 1993

Yoshimi KASUGAI*, Akihiko TANAKA*, Masato ASAI*
Hiroshi YAMAMOTO*, Toshio KATOH*, Toshiyuki IIDA**
Akito TAKAHASHI** and Kiyoshi KAWADE*

日 本 原 子 力 研 究 所
Japan Atomic Energy Research Institute

JAERI-Mレポートは，日本原子力研究所が不定期に公刊している研究報告書です。
入手の問合わせは，日本原子力研究所技術情報部情報資料課（〒319-11茨城県那珂郡東海村）あて，お申しこしください。なお，このほかに財団法人原子力弘済会資料センター（〒319-11 茨城県那珂郡東海村日本原子力研究所内）で複写による実費頒布をおこなっております。

JAERI-M reports are issued irregularly.
Inquiries about availability of the reports should be addressed to Information Division Department of Technical Information, Japan Atomic Energy Research Institute, Tokai-mura, Naka-gun, Ibaraki-ken 319-11, Japan.

編集兼発行　日本原子力研究所
印　　刷　いばらき印刷㈱

JAERI-M 93-124

Measurement of Formation Cross Sections of Short-lived Nuclei by 14 MeV Neutrons - Ru, Pd, Cd, Sn -

Yoshimi KASUGAI*, Akihiko TANAKA*, Masato ASAI*
Hiroshi YAMAMOTO*, Toshio KATOH*, Toshiyuki IIDA**
Akito TAKAHASHI** and Kiyoshi KAWADE*

Department of Reactor Engineering
Tokai Research Establishment
Japan Atomic Energy Research Institute
Tokai-mura, Naka-gun, Ibaraki-ken

(Received May 21, 1993)

Eighteen neutron activation for (n,2n), (n,p), (n,n'p) and (n,α) reactions producing short-lived nuclei with half-lives between 21 s and 21 min have been measured in the energy range of 13.4 to 14.9 MeV for Ru, Pd, Cd and Sn.

Half-life of ^{105m}Rh, ^{120m1}In and ^{120m2}In produced by 14 MeV neutron bombardments was measured with Ge detectors in the spectrum multi-scaling mode.

Keywords: Activation, Cross Section, 14 MeV Neutron, Short-lived Nucleus, Half-life, Measurement, Ge Detector

---

This work was performed under the contract between Japan Atomic Energy Research Institute and Nagoya University.

* Nagoya University

** Osaka University

14MeV 中性子による短寿命核生成断面積の測定
－Ru, Pd, Cd, Sn－

日本原子力研究所東海研究所原子炉工学部
春日井好己* ・田中　晶彦* ・浅井　雅人*
山本　　洋* ・加藤　敏郎* ・飯田　敏行**
高橋　亮人** ・河出　　清*

（1993年5月21日受理）

半減期が21分から21秒程度の短寿命核生成断面積を，中性子エネルギー13.4から14.9MeVの範囲にわたり，Ru，Pd，Sn，Cdの（n,2n），（n,p），(n,α），(n,n'p）反応のうち，18反応を測定した。

また，14MeV中性子で生成される短寿命核の半減期の測定を，^{105m}Rh，^{120m1}In，^{120m2}In，の3核種に対して，Ge検出器を用いてスペクトルマルチスケーリングモードで行った。

本報告書は，日本原子力研究所が名古屋大学に委託して行った研究の成果である。

東海研究所：〒319-11　茨城県那珂郡東海村白方字白根2-4

* 名古屋大学

**大阪大学

Contents

目　　次

1. Introduction

Neutron activation cross section data around 14 MeV have become important from the viewpoint of fusion reactor technology, especially for calculations on radiation damage, nuclear transmutation, induced activity and so on.

In recent years formation cross sections of long−lived nuclei were measured systematically in a good accuracy[1]. However there remain many short−lived nuclei whose cross sections have not been measured yet or have not been measured in a reasonable accuracy because of difficulty in measurement for short−lived nuclei.

A measuring program for activation cross sections of short−lived nuclei around 14 MeV neutrons has been carried out at the intense 14 MeV neutron source facility (OKTAVIAN) of Osaka University since 1988. Up to now, we have measured 47 cross sections for the (n, 2n), (n, p), (n, n'p) and (n, α) reactions leading to short−lived nuclei in a qualified experimental condition[2−4].

In this work 18 cross sections producing short lived nuclei ($T_{1/2}$= 21 s − 22 min) were measured in the energy range from 13.4 MeV to 14.9 MeV for Ru, Pd, Cd and Sn. Measured reactions are shown in Table 1.

Half−life of three short−lived nuclei was measured with Ge detectors in the spectrum multi−scaling mode. These values are needed for the cross section determination. The measured half−lives are shown in Table 2.

2. Measurement of activation cross sections

The activation cross section values were obtained by measuring the radioactivities induced with neutron irradiation as follows:

$$C = N\sigma\phi\varepsilon_f I\gamma(1-\exp(-\lambda t_i))\exp(-\lambda t_c)(1-\exp(-\lambda t_m))/\lambda$$

where

C : γ−ray peak counts,
N : atomic number of target nuclide,
σ : activation cross section measured,
ϕ : neutron flux at the irradiation position,

1. Introduction

Neutron activation cross section data around 14 MeV have become important from the viewpoint of fusion reactor technology, especially for calculations on radiation damage, nuclear transmutation, induced activity and so on.

In recent years formation cross sections of long-lived nuclei were measured systematically in a good accuracy[1]. However there remain many short-lived nuclei whose cross sections have not been measured yet or have not been measured in a reasonable accuracy because of difficulty in measurement for short-lived nuclei.

A measuring program for activation cross sections of short-lived nuclei around 14 MeV neutrons has been carried out at the intense 14 MeV neutron source facility (OKTAVIAN) of Osaka University since 1988. Up to now, we have measured 47 cross sections for the (n, 2n), (n, p), (n, n'p) and (n, α) reactions leading to short-lived nuclei in a qualified experimental condition[2-4].

In this work 18 cross sections producing short lived nuclei ($T_{1/2}$= 21 s - 22 min) were measured in the energy range from 13.4 MeV to 14.9 MeV for Ru, Pd, Cd and Sn. Measured reactions are shown in Table 1.

Half-life of three short-lived nuclei was measured with Ge detectors in the spectrum multi-scaling mode. These values are needed for the cross section determination. The measured half-lives are shown in Table 2.

2. Measurement of activation cross sections

The activation cross section values were obtained by measuring the radioactivities induced with neutron irradiation as follows:

$$C = N\sigma\phi\varepsilon_f I\gamma(1-\exp(-\lambda t_i))\exp(-\lambda t_c)(1-\exp(-\lambda t_m))/\lambda$$

where

C : γ-ray peak counts,
N : atomic number of target nuclide,
σ : activation cross section measured,
ϕ : neutron flux at the irradiation position,

ε_f : full energy peak detection efficiency of γ−ray,
Iγ : γ−ray emission probability per disintegration,
λ : decay constant of induced radioactivity,
t_i : irradiation time,
t_c : cooling time,
t_m: measuring time of γ−ray.

All cross section values were obtained relative to the standard reaction cross section of $^{27}Al(n, \alpha)^{24}Na$ (ENDF/B−V)[5].

2.1 Experimental

2.1.1 Neutron irradiation and fluence monitoring

The d−T neutrons were generated by an intense 14 MeV neutron source facility (OKTAVIAN) of Osaka University. Incident d^+ beam energy and intensity were 300 keV and about 5 mA, respectively. A pneumatic sample transport system as shown in Fig. 1 was used for the irradiation of samples. The angles of the irradiation position to the d^+ beam were 0°, 50°, 75°, 105°, 125° and 155°, which covered the neutron energies ranging from 14.9 to 13.4 MeV. Another pneumatic tube was also set at −105°. The distance between the T−target and the irradiation position was 15 cm. When high neutron flux was required, an additional tube set at 0° and at 1.5 cm was used. Typical neutron fluxes at each position are shown in Fig. 2. The neutron flux at 75° was a little low owing to neutron scattering with the rotating T−target assembly.

The neutron flux at the sample position was measured with use of the substandard $^{27}Al(n, p)^{27}Mg$ ($T_{1/2}$= 9.46 min) reaction, whose cross sections were determined by referring to the standard $^{27}Al(n, \alpha)^{24}Na$ (ENDF/B−V). The samples were sandwiched between two aluminum foils of 10 mm × 10 mm × 0.2 mm thick. The standard cross section of $^{27}Al(n, \alpha)$ is shown in Table 3. Good statistics for fluence monitoring could be achieved in reasonably short measuring time by using the $^{27}Al(n, p)$ reaction instead of $^{27}Al(n, \alpha)$. The use of the substandard $^{27}Al(n, p)$ reaction brought only an additional statistical uncertainty of 0.5% to final results.

The effective energy of incident neutrons at each irradiation position was determined by the ratio of the $^{90}Zr(n, 2n)^{89}Zr$(3.27 d)[6] and $^{93}Nb(n, 2n)^{92m}Nb$ (10.15

d)[7] cross sections (Zr/Nb method[8]). Since each position of the pneumatic tubes was mutually arranged in a good accuracy, the effective d^+ energy was chosen as a fitting parameter in the relativistic calculation of d–T neutron energy. A fitting result obtained for E_d = 130 keV is shown in Fig. 3. The uncertainty in the neutron energy was estimated to be 50 keV.

Mass separated isotopes from the Oak Ridge National Laboratory were used as samples. Powder samples were wrapped in powder papers (each sample size: 10 mm × 10 mm and about 1 mm thick, sample masses: 20–70 mg). The isotopic compositions of samples used are shown in Table 4.

2.1.2 Activity measurement

Gamma–rays emitted from the irradiated samples and monitor aluminum foils were measured with 12% and 4% HPGe detectors, and a 16% HPGe detector, respectively. Foils of Nb and Zr for neutron energy determination were measured with a 22% HPGe detector. The Ge detectors used are shown in Table 5. Each detector was covered with a 5 mm thick acrylic absorber in order to reduce β–rays. The peak efficiency calibration at 5 cm was accomplished by using sources of ^{24}Na, ^{56}Co, ^{133}Ba, ^{152}Eu and ^{154}Eu. Corrections for true coincidence sums were applied. The errors in the efficiency curves were estimated to be 1.5% above 300 keV, 3% between 300 and 80 keV, and 5% below 80 keV.

To measure the weak activities efficiently, the samples were put on the absorber surface (source–to–detector distance is 5 mm). To convert the efficiency at 5 mm to the one at 5 cm, calibration measurements were carried out at both distances by using extra samples irradiated with rather strong neutron flux through the pneumatic tube set at 1.5 cm. This method improved the detection efficiency by a factor of about 7. The calibration procedure brought an additional error of 1.0% to the results.

Peak areas of the γ–rays were evaluated by summing all recorded counts in the channel interval {C−3σ, C+3σ} and subtracting the background counts (N_B), where C is the position of the peak center and σ is FWHM. N_B is given by (6σ) × $(N_L + N_H)/2$, where N_L and N_H are the average counts of 5 channels in the vicinity of (C−3σ) and (C+3σ), respectively. In Fig. 4, the peak area evaluation of the 215 keV γ–ray emitted by ^{107m}Pd produced by $^{108}Pd(n, 2n)^{107m}Pd$ reaction is shown as an example. This summing method is similar to that by Debertin and

Schötzig[9]. The uncertainty from the peak area evaluation was estimated to be 0.5%.

2.1.3 Decay data

In Table 6, measured reactions and associated decay data[10] of the half−life ($T_{1/2}$), the γ−ray energy (Eγ) and the absolute intensity in photons per disintegration (Iγ) are listed together with the Q values. The half−life of ^{105m}Rh, ^{120m1}In and ^{120m2}In was determined in this work.

2.1.4 Corrections

The following principal corrections in deducing cross sections were made:

1) fluctuation of the neutron flux during the irradiation,
2) contribution of scattered low energy neutrons,
3) true coincidence sum,
4) random coincidence sum,
5) deviation in the measuring position coming from different thickness of each sample,
6) self−absorption of the γ−ray in the sample material,
7) interfering reaction producing activities emitting the γ−ray with the same energy of interest.

The detailed procedures are described elsewhere[2,3].

2.1.5 Error Estimation

The total errors (δ_t) were derived by combining the experimental error (δ_e) and the error of nuclear data (δ_r) in quadratic: $\delta_t^2 = \delta_e^2 + \delta_r^2$. Estimated major sources of the error are listed in Table 7. When good counting statistics were achieved, the experimental and total errors were 2.4 and 6.0%, respectively. The main error sources are due to the γ−ray detection efficiency and the standard ^{27}Al(n, α)^{24}Na reaction cross section. In some cases the errors of the γ−ray emission probability or the half−life were dominant. When the error of nuclear data is reduced, the total error will be much improved.

2.2 Results and discussion

Numerical data tables of the cross sections are given in Table 8 and the

d)[7] cross sections (Zr/Nb method[8]). Since each position of the pneumatic tubes was mutually arranged in a good accuracy, the effective d^+ energy was chosen as a fitting parameter in the relativistic calculation of d–T neutron energy. A fitting result obtained for E_d = 130 keV is shown in Fig. 3. The uncertainty in the neutron energy was estimated to be 50 keV.

Mass separated isotopes from the Oak Ridge National Laboratory were used as samples. Powder samples were wrapped in powder papers (each sample size: 10 mm × 10 mm and about 1 mm thick, sample masses: 20–70 mg). The isotopic compositions of samples used are shown in Table 4.

2.1.2 Activity measurement

Gamma–rays emitted from the irradiated samples and monitor aluminum foils were measured with 12% and 4% HPGe detectors, and a 16% HPGe detector, respectively. Foils of Nb and Zr for neutron energy determination were measured with a 22% HPGe detector. The Ge detectors used are shown in Table 5. Each detector was covered with a 5 mm thick acrylic absorber in order to reduce β–rays. The peak efficiency calibration at 5 cm was accomplished by using sources of ^{24}Na, ^{56}Co, ^{133}Ba, ^{152}Eu and ^{154}Eu. Corrections for true coincidence sums were applied. The errors in the efficiency curves were estimated to be 1.5% above 300 keV, 3% between 300 and 80 keV, and 5% below 80 keV.

To measure the weak activities efficiently, the samples were put on the absorber surface (source–to–detector distance is 5 mm). To convert the efficiency at 5 mm to the one at 5 cm, calibration measurements were carried out at both distances by using extra samples irradiated with rather strong neutron flux through the pneumatic tube set at 1.5 cm. This method improved the detection efficiency by a factor of about 7. The calibration procedure brought an additional error of 1.0% to the results.

Peak areas of the γ–rays were evaluated by summing all recorded counts in the channel interval {C−3σ, C+3σ} and subtracting the background counts (N_B), where C is the position of the peak center and σ is FWHM. N_B is given by (6σ) × $(N_L + N_H)/2$, where N_L and N_H are the average counts of 5 channels in the vicinity of (C−3σ) and (C+3σ), respectively. In Fig. 4, the peak area evaluation of the 215 keV γ–ray emitted by ^{107m}Pd produced by $^{108}Pd(n, 2n)^{107m}Pd$ reaction is shown as an example. This summing method is similar to that by Debertin and

Schötzig[9]. The uncertainty from the peak area evaluation was estimated to be 0.5%.

2.1.3 Decay data

In Table 6, measured reactions and associated decay data[10] of the half-life ($T_{1/2}$), the γ-ray energy (Eγ) and the absolute intensity in photons per disintegration (Iγ) are listed together with the Q values. The half-life of ^{105m}Rh, ^{120m1}In and ^{120m2}In was determined in this work.

2.1.4 Corrections

The following principal corrections in deducing cross sections were made:

1) fluctuation of the neutron flux during the irradiation,
2) contribution of scattered low energy neutrons,
3) true coincidence sum,
4) random coincidence sum,
5) deviation in the measuring position coming from different thickness of each sample,
6) self-absorption of the γ-ray in the sample material,
7) interfering reaction producing activities emitting the γ-ray with the same energy of interest.

The detailed procedures are described elsewhere[2,3].

2.1.5 Error Estimation

The total errors (δ_t) were derived by combining the experimental error (δ_e) and the error of nuclear data (δ_r) in quadratic: $\delta_t^2 = \delta_e^2 + \delta_r^2$. Estimated major sources of the error are listed in Table 7. When good counting statistics were achieved, the experimental and total errors were 2.4 and 6.0%, respectively. The main error sources are due to the γ-ray detection efficiency and the standard ^{27}Al(n, α)^{24}Na reaction cross section. In some cases the errors of the γ-ray emission probability or the half-life were dominant. When the error of nuclear data is reduced, the total error will be much improved.

2.2 Results and discussion

Numerical data tables of the cross sections are given in Table 8 and the

measured data are compared to other data in Fig.5. In the figures the total errors are shown.

For the following four reactions the cross sections were measured for the first time: ^{102}Ru(n, np)^{101}Tc, ^{105}Pd(n, np)^{104m}Rh, ^{106}Pd(n, np)^{105m}Rh and ^{112}Cd(n, α)^{109m}Pd. No previous works on these reactions might be made due to too small cross sections (less than 5 mb). The previous cross section data of ^{101}Ru(n, p)^{101}Tc[11], ^{108}Pd(n, np)^{107}Rh[12], ^{116}Cd(n, p)^{116g}Ag[13] and ^{119}Sn(n, p)^{119g}In[14] are discrepant with the present values by a factor of more than 2. In particular the cross section of ^{101}Ru(n, p) reaction measured by Paul and Clarke[11]is discrepant with the present values by a factor of more than 10. In Fig. 5.1 the present cross section data of ^{101}Ru(n, p) are shown together with the previous and estimated values based on the systematics proposed by us[15]. The systematics is expressed by the following formula:

$$\sigma_{n,p}(mb)=(6.0\times10^{-4})A^{5.7}(0.585)^{(\ln A)^2}\exp\{-33(N-Z)/A+\delta\}$$

$$\delta=\begin{cases} 0 & (e\text{-}e\ \textit{target nucleus}) \\ +0.15 & (e\text{-}o) \\ -0.15 & (o\text{-}e) \end{cases}$$

where N, Z and A are neutron, proton and the mass number of the target nuclei. The present values of this reaction cross section are consistent with our systematics.

The cross section data of ^{102}Ru(n, p)^{102m}Tc, ^{104}Ru(n, p)^{104}Tc and ^{104}Ru(n, α)^{101}Mo by Gray et al.[16] agree with the present data within the uncertainties, but his data show systematically low values compared with the present data. The induced radioactivities produced by these reactions emit cascade γ−rays. In our measurement the true coincidence−sum corrections ranged between 15% and 30 % at 5 mm. His lower values might result from insufficient corrections.

For ^{120m}In produced by the reaction ^{120}Sn(n, p)^{120m}In the existence of two isomers with similar half−lives was recognized[17]. In this work the formation cross sections of two isomers, ^{120m1,2}In, were separately measured. The previous values of the ^{120}Sn(n,p)^{120m}In cross sections were measured without the separation of the decay of two isomers ^{120m}In. The previous values of ^{108}Pd(n,2n)^{107m}Pd[18,19] cross section agree well with the present value.

In appendix 1, the singles γ−ray spectra of the samples irradiated by 14 MeV

neutrons are shown.

3. Measurement of half-lives

The half-life value is one of the important decay data for cross section measurement. It is therefore required that the half-life values are precise and reliable. The error of the ^{105m}Rh half-life previously reported[20] was not evaluated. It had been considered ^{120}In had one isomer with a half-life of 44.4 s[10]. Cheung et al. found ^{120m}In had two components[17]. It was determined by them that one half-life (^{120m1}In) was 47.3(5) s and another (^{120m2}In) 46.2(8) s.

We measured the half-lives of ^{105m}Rh and of two isomers of ^{120}In. These values are needed for cross section determination. The γ-rays were measured with the Ge detector in the spectrum multi-scaling mode. The measurement was made at equal interval of 1/3 to 1/6 of the half-life for about 10 times the half-life. The ^{137}Cs, ^{170}Tm and ^{241}Am sources and a pulse generator with a rate of 60 cps were simultaneously measured together with the short-lived activity for the correction of the pile-up and the dead time losses (source method, constant-pulser method). The initial counting rates were always kept to be less than 9×10^3 cps. Data points were analyzed by the least squares fitting. The detailed procedures are described elsewhere[21].

The results are summarized in Table 9 together with the production reactions, followed γ-rays, reference sources for corrections and previous data. The results are shown in Fig. 6 together with the previous works. As an example, singles γ-ray spectrum and the decay curve of ^{105m}Rh are shown in Fig. 7 and Fig. 8, respectively.

Previous values of these half-lives are longer by 6-4% than the present values. This might be due to insufficient corrections of the pile-up and the dead time losses.

4. Summary

The activation cross sections were measured on the 18 reactions producing the

neutrons are shown.

3. Measurement of half-lives

The half-life value is one of the important decay data for cross section measurement. It is therefore required that the half-life values are precise and reliable. The error of the ^{105m}Rh half-life previously reported[20] was not evaluated. It had been considered ^{120}In had one isomer with a half-life of 44.4 s[10]. Cheung et al. found ^{120m}In had two components[17]. It was determined by them that one half-life (^{120m1}In) was 47.3(5) s and another (^{120m2}In) 46.2(8) s.

We measured the half-lives of ^{105m}Rh and of two isomers of ^{120}In. These values are needed for cross section determination. The γ-rays were measured with the Ge detector in the spectrum multi-scaling mode. The measurement was made at equal interval of 1/3 to 1/6 of the half-life for about 10 times the half-life. The ^{137}Cs, ^{170}Tm and ^{241}Am sources and a pulse generator with a rate of 60 cps were simultaneously measured together with the short-lived activity for the correction of the pile-up and the dead time losses (source method, constant-pulser method). The initial counting rates were always kept to be less than 9×10^3 cps. Data points were analyzed by the least squares fitting. The detailed procedures are described elsewhere[21].

The results are summarized in Table 9 together with the production reactions, followed γ-rays, reference sources for corrections and previous data. The results are shown in Fig. 6 together with the previous works. As an example, singles γ-ray spectrum and the decay curve of ^{105m}Rh are shown in Fig. 7 and Fig. 8, respectively.

Previous values of these half-lives are longer by 6-4% than the present values. This might be due to insufficient corrections of the pile-up and the dead time losses.

4. Summary

The activation cross sections were measured on the 18 reactions producing the

neutrons are shown.

3. Measurement of half-lives

The half-life value is one of the important decay data for cross section measurement. It is therefore required that the half-life values are precise and reliable. The error of the ^{105m}Rh half-life previously reported[20] was not evaluated. It had been considered ^{120}In had one isomer with a half-life of 44.4 s[10]. Cheung et al. found ^{120m}In had two components[17]. It was determined by them that one half-life (^{120m1}In) was 47.3(5) s and another (^{120m2}In) 46.2(8) s.

We measured the half-lives of ^{105m}Rh and of two isomers of ^{120}In. These values are needed for cross section determination. The γ-rays were measured with the Ge detector in the spectrum multi-scaling mode. The measurement was made at equal interval of 1/3 to 1/6 of the half-life for about 10 times the half-life. The ^{137}Cs, ^{170}Tm and ^{241}Am sources and a pulse generator with a rate of 60 cps were simultaneously measured together with the short-lived activity for the correction of the pile-up and the dead time losses (source method, constant-pulser method). The initial counting rates were always kept to be less than 9×10^3 cps. Data points were analyzed by the least squares fitting. The detailed procedures are described elsewhere[21].

The results are summarized in Table 9 together with the production reactions, followed γ-rays, reference sources for corrections and previous data. The results are shown in Fig. 6 together with the previous works. As an example, singles γ-ray spectrum and the decay curve of ^{105m}Rh are shown in Fig. 7 and Fig. 8, respectively.

Previous values of these half-lives are longer by 6-4% than the present values. This might be due to insufficient corrections of the pile-up and the dead time losses.

4. Summary

The activation cross sections were measured on the 18 reactions producing the

short-lived nuclei in the neutron energy range of 13.4 to 14.9 MeV for Ru, Pd, Cd and Sn by the activation method. The half-life of ^{120m1}In, ^{120m2}In and ^{105m}Rh was measured by applying both the source and pulser methods.

Acknowledgments

This work was performed under the contract between Nagoya University and Japan Atomic Energy Research Institute.

The authors wish to express their sincere thanks to Dr. Y. Nakajima of the JAERI Nuclear Data Center. They are also grateful to Prof. K. Sumita for his support to this work and Messrs. H. Sugimoto, J. Datemichi and S. Yoshida for the operation of the OKTAVIAN accelerator.

short-lived nuclei in the neutron energy range of 13.4 to 14.9 MeV for Ru, Pd, Cd and Sn by the activation method. The half-life of ^{120m1}In, ^{120m2}In and ^{105m}Rh was measured by applying both the source and pulser methods.

Acknowledgments

This work was performed under the contract between Nagoya University and Japan Atomic Energy Research Institute.

The authors wish to express their sincere thanks to Dr. Y. Nakajima of the JAERI Nuclear Data Center. They are also grateful to Prof. K. Sumita for his support to this work and Messrs. H. Sugimoto, J. Datemichi and S. Yoshida for the operation of the OKTAVIAN accelerator.

References

1) Y. Ikeda, C. Konno, K. Oishi, T. Nakamura, H. Miyade, K. Kawade, H. Yamamoto and T. Katoh: JAERI 1312 (1988).
2) T. Katoh, K. Kawade and H. Yamamoto: JAERI-M 89-083 (1989) (in Japanese).
3) K. Kawade, H. Yamamoto, T. Yamada, T. Katoh, T. Iida and A. Takahashi: JAERI-M 90-171 (1990).
4) K. Kawade, H. Yamamoto, T. Kobayashi, T. Katoh, T. Iida and A. Takahashi: JAERI-M 92-020 (1992).
5) "Evaluated Neutron Data File, ENDF/B-V", ENDF/B Summary Documentation, compiled by R. Kinsey, ENDF-201, 3rd edition, Brookhaven Laboratory (1979).
6) A. Pavlik, G. Winkler, H. Vonach, A. Paulsen and H. Liskien: J. Phys. G; Nucl. Phys. 8, 1283 (1982).
7) D.R. Nethaway: J. Inorg. Nucl. Chem. 40, 1285 (1978).
8) V.E. Lewis and K.J. Zieba: Nucl. Instr. Meth. 174, 141 (1980).
9) K. Debertin and U. Schötzig: Nucl. Instr. Meth. 140, 337 (1977).
10) E. Browne, R.B. Firestone and V.S. Shirley: "Table of Radioactive Isotopes", John Wiley & Sons, New York (1986).
11) E.B. Paul and R.L. Clarke: Can. J. Phys. 31, 267 (1953).
12) J.F. Barry, R.F. Coleman, B.E. Hawker and J.L. Perkin: Proc. Phys. Soc. 74, 632(1959)
13) Y.W. Yu and D.G. Gardner: Nucl. Phys. A98, 451 (1967)
14) S. Lulic, P. Strol, B. Antolkovic and G. Paic: Nucl. Phys. A119 517 (1968).
15) Y. Kasugai, H. Yamamoto, A. Takahashi, T. Iida and K. Kawade: JAERI-M 93-046, 277 (1993)
16) P.R. Gray, A.R. Zander and T.G. Ebrey: Nucl. Phys. 75, 215(1966).
17) H.C. Cheung, H. Huanr, B.N. Subba Rao, L. Lessard and J.K. Lee: J. Phys. G; Nucl. Phys. 4, 1501 (1978)
18) B. Minetti and A. Pasquarell: Nucl. Phys. A118, 449 (1968)
19) W.D. Lu and R.W. Fink: Bull. Am. Phys.: Nucl. Phys. 31, 1422 (1968).
20) R.B. Duffield and L.M. Langer: Phys. Rev. 81, 203 (1951)
21) M. Miyachi, H. Ukon, M. Shibata, Y. Gotoh, H. Yamamoto, K. Kawade, T. Katoh, T. Iida and A. Takahashi: Proc. Nucl. Data for Sci. and Tech. (1988, Mito) 897.

Table 1 Measured reactions

Reaction[a]	$T_{1/2}$	Reaction	$T_{1/2}$
$^{101}Ru(n,p)^{101}Tc$	14.2 min	$^{108}Pd(n,2n)^{107m}Rd$	21.3 s
$^{102}Ru(n,p)^{102m}Tc$	4.35 min	$(n,p)^{108g}Rh$	6.0 min
$(n,np)^{101}Tc$	14.2 min	$(n,np)^{107}Rh$	21.7 min
$^{104}Ru(n,p)^{104}Tc$	18.3 min	$^{112}Cd(n,\alpha)^{109m}Pd$	4.69 min
$(n,\alpha)^{101}Mo$	14.6 min	$^{116}Cd(n,p)^{116g}Ag$	2.68 min
$^{104}Pd(n,p)^{104m}Rh$	4.34 min	$^{119}Sn(n,p)^{119g}In$	2.4 min
$^{105}Pd(n,p)^{105m}Rh$	42.4 s[b]	^{119m}In	18.0 min
$(n,np)^{104m}Rh$	4.34 min	$^{120}Sn(n,p)^{120m1}In$[c]	43.5 s[b]
$^{106}Pd(n,np)^{105m}Rh$	42.4 s	$^{120m2}In$[c]	45.6 s[b]

a) (n,np) means [(n,d)+(n,n'p)+(n,pn)].

b) Measurd in the present work.

c) It was shown that ^{120}In had two isomers in ref. 17. $^{120m1}In$ is a low-spin isomer (3^+, 4^+, 5^+), and $^{120m2}In$ is a high-spin isomer (8^-).

Table 2 Measured half-lives

Nuclide (half-life)		
^{105m}Rh (42 s)	$^{120m1}In$ (44 s)	$^{120m2}In$ (46 s)

Table 3 Cross section of $^{27}Al(n,\alpha)\ ^{24}Na$ reaction[a)]

En(MeV)	Cross section(mb)
14.96	113.42
14.92	113.93
14.84	114.97
14.71	116.65
14.53	118.97
14.32	121.28
14.10	123.63
13.95	125.02
13.81	125.93
13.68	126.77
13.55	127.62
13.33	128.60

a) Taken from ENDF/B-V. Uncertainty is ±3% for all values.

Table 4 Samples of enriched isotopes[a)]

Sample	Chemical form	Enrichment (%)	Weight (mg)	Reaction	Isotopic composition Mass Number(atomic percent)
^{101}Ru	Ru	96.03	60	^{101}Ru(n,p)	99(0.24), 100(0.64) 102(2.73), 104(0.36)
^{102}Ru	Ru	98.95	47	^{102}Ru(n,p)^{m} (n,np)	99(0.12), 100(0.15) 101(0.37), 104(0.41)
^{104}Ru	Ru	99.05	37	^{104}Ru(n,p) (n,α)	99(0.10), 100(0.13) 101(0.23), 102(0.49)
^{104}Pd	Pd	96.02	16	^{104}Pd(n,p)^{m}	105(4.48), 106(1.15) 108(0.79), 110(0.56)
^{105}Pd	Pd	96.58	30	^{105}Pd(n,p)^{m} (n,np)^{m}	104(0.41), 106(2.35) 108(0.46), 110(0.20)
^{106}Pd	Pd	97.51	38	^{106}Pd(n,np)^{m}	104(0.24), 105(1.00) 108(0.72), 110(0.53)
^{108}Pd	Pd	98.79	38	^{108}Pd(n,2n)^{m} (n,p)^{g},(n,np)	104(0.15), 105(0.31) 106(0.39), 110(0.36)
^{112}Cd	CdO	97.26	58	^{112}Cd(n,α)^{m}	106(0.02), 108(0.02) 110(0.26), 111(0.63) 113(0.88), 114(0.85) 116(0.08)
^{116}Cd	CdO	94.97	43	^{116}Cd(n,p)^{g}	106(0.07), 108(0.02) 110(0.24), 111(0.58) 112(0.74), 113(0.73) 114(2.65)
^{119}Sn	SnO_2	84.48	65	^{119}Sn(n,p)^{m,g}	116(0.40), 117(0.85) 118(3.63), 120(9.98) 122(0.44), 124(0.20)
^{120}Sn	SnO_2	98.05	70	^{120}Sn(n,p)^{m1,2}	116(0.13), 117(0.11) 118(0.61), 119(0.66) 122(0.34), 124(0.10)

a) Enriched isotopes were obtained from the Oak Ridge National Laboratory.

Table 5 Ge detectors used for cross section measurement

Detector	Volume (cm^3)	Efficiency (%)	FWHM[a)] (keV)	Object of measurement
p-type HPGe	60	12	1.75	Short-lived nuclei
n-type HPGe	30	4	0.61[b)]	Short-lived nuclei
n-type HPGe	89	16	2.00	Al monitor foil(^{27}Mg)
p-type HPGe	102	22	1.65	Neutron energy calibration (Nb, Zr foils)

a) at 1333 keV
b) at 122 keV

Table 6 Measured reactions and decay parameters[a)]

Reaction[b)]	$T_{1/2}$	Eγ(keV)	Iγ(%)	Q(MeV)[c)]
$^{101}Ru(n,p)^{101}Tc$	14.2(1) min	306.8	88(4)	-0.84
$^{102}Ru(n,p)^{102m}Tc$	4.35(7) min	475.1	85.3(20)	-3.74
$(n,np)^{101}Tc$	14.2(1) min	306.8	88(4)	-10.1
$^{104}Ru(n,p)^{104}Tc$	18.3(3) min	358.0	79(10)	-4.83
$(n,\alpha)^{101}Mo$	14.6(1) min	191.9	18.8(10)	1.06
$^{104}Pd(n,p)^{104m}Rh$	4.34(5) min	51.4	48.3(5)	-1.79
$^{105}Pd(n,p)^{105m}Rh$	42.4(5) s[d)]	129.6	20.0(4)	0.086
$(n,np)^{104m}Rh$	4.34(5) min	51.4	48.3(5)	-8.88
$^{106}Pd(n,np)^{105m}Rh$	42.4(5) s[d)]	129.6	20.0(4)	-9.35
$^{108}Pd(n,2n)^{107m}Pd$	21.3(5) s	214.9	69.0(29)	-9.43
$(n,p)^{108g}Rh$	6.0(3) min	581.0	59(12)	-3.65
$(n,np)^{107}Rh$	21.7(4) min	302.8	66(5)	-9.95
$^{112}Cd(n,\alpha)^{109m}Pd$	4.69(1) min	188.9	55.8(7)	2.48
$^{116}Cd(n,p)^{116g}Ag$	2.68(1) min	513.5	76(4)	-5.21
$^{119}Sn(n,p)^{119g}In$	2.4(1) min	763.1	99.08(15)	-1.55
^{119m}In	18.0(3) min	311.4	0.99(20)	-1.86
$^{120}Sn(n,p)^{120m1}In$[e)]	43.5(8) s[d)]	1171.3	96.1(10)	-4.52
$^{120m2}In$[e)]	48.4(4) s[d)]	197.1	80.6(31)	-4.52
$^{27}Al(n.\alpha)^{24}Na$ [f)]	14.959 h	1368.6	99.994(3)	-3.13
$^{27}Al(n,p)^{27}Mg$ [g)]	9.46 min	843.8	72.0(4)	-1.83

a)Taken from ref.10.

b)(n,np) means [(n,d)+(n,n'p)+(n,pn)]

c)Q(n,n'p) is given here. Q(n,d)=Q(n,n'p)+2.225 MeV.

d)Measured in this work.

e)See ref. 17.

f)Standard reaction(ENDF/B-V) used in this work.

g)Secondary standard reaction used for short-lived nuclei.

Table 7 Principal sources of uncertainty in the measured cross sections

Experimental error (δ_e)	
Source of error	Uncertainty(%)
Counting statistics	0.5 - 29
Sample mass including purity	0.1
Neutron flux fluctuation	< 0.1 (20% of correction)
Gamma-peak area evaluation	0.5
Detector efficiency	1.5 (Eγ > 300keV)
	3 (300-80 keV)
	5 (Eγ < 80 keV)
Efficiency calibration at 0.5 and 5 cm	2.0
Correction for	
true coincidence sum	< 17
random coincidence sum	< 0.4
sample thickness	0.6-1.4 (20% of correction)
self-absorption of γ-rays	0-2.6 (20% of correction)
low energy neutrons	0.7 (30-40% of correction)
Secondary reference cross section for $^{27}Al(n,p)^{27}Mg$	0.5(Only statistics)

Error of nuclear data(δ_r)	
Source of error	Uncertainty(%)
Reference cross section $^{27}Al(n,\alpha)^{24}Na$ (ENDF/B-V)	3.0
Absolute γ-ray intensity	0-20
Half-life	0-5

Table 8(a) Activation cross section of short-lived nuclei

$^{101}Ru(n,p)^{101}Tc$ (14.2 min)					$^{102}Ru(n,p)^{102m}Tc$ (4.35 min)			
En(MeV)	σ(mb)	δ_e(%)	δ_r(%)	δ_t(%)	σ(mb)	δ_e(%)	δ_r(%)	δ_t(%)
14.87	25.1	2.4	5.5	6.0	9.5	8.6	4.1	9.5
14.58	25.0	2.4	5.5	6.0	8.8	8.7	4.1	9.6
14.28	22.5	2.5	5.5	6.1	7.5	8.8	4.1	9.7
13.88	20.5	2.4	5.5	6.0	7.1	8.6	4.1	9.5
13.65	19.3	2.5	5.5	6.0	6.3	8.8	4.1	9.7
13.40	18.3	2.4	5.5	6.0	5.6	8.7	4.1	9.6
$^{102}Ru(n,np)^{101}Tc$ (14.2 min)					$^{104}Ru(n,p)^{104}Tc$ (18.3 min)			
En(MeV)	σ(mb)	δ_e(%)	δ_r(%)	δ_t(%)	σ(mb)	δ_e(%)	δ_r(%)	δ_t(%)
14.87	2.95	4.0	5.5	6.8	8.3	5.1	11	12
14.58	2.21	4.3	5.5	7.0	8.0	5.5	11	12
14.28	1.47	5.6	5.5	7.9	6.8	5.6	11	12
13.88	0.94	5.9	5.5	8.1	5.6	5.3	11	12
13.65	0.71	7.6	5.5	9.4	5.1	6.9	11	12
13.40	0.58	8.4	5.5	10	4.3	5.7	11	12
$^{104}Ru(n,\alpha)^{101}Mo$ (14.6 min)					$^{104}Pd(n,p)^{104m}Rh$ (4.34 min)			
En(MeV)	σ(mb)	δ_e(%)	δ_r(%)	δ_t(%)	σ(mb)	δ_e(%)	δ_r(%)	δ_t(%)
14.87	3.1	10	6.2	12	19.2	5.9	3.4	6.8
14.58	3.5	13	6.2	14	19.6	5.6	3.4	6.5
14.28	2.8	14	6.2	15	19.0	5.7	3.4	6.6
13.88	2.4	11	6.2	12	17.2	5.5	3.4	6.4
13.65	1.8	25	6.2	26	16.4	5.5	3.4	6.5
13.40	1.7	14	6.2	15	15.3	5.6	3.4	6.5
$^{105}Pd(n,p)^{105m}Rh$(42.4 s)					$^{105}Pd(n,np)^{104m}Rh$(4.34 min)			
En(MeV)	σ(mb)	$\delta_{e(\%)}$	δ_r(%)	δ_t(%)	σ(mb)	$\delta_{e(\%)}$	δ_r(%)	$\delta_{t(\%)}$
14.87	15.7	8.5	3.8	9.3	4.91	6.3	3.4	7.2
14.58	12.9	9.2	3.8	9.9	3.74	6.6	3.4	7.4
14.28	14.3	9.6	3.8	10	2.59	7.0	3.4	7.8
13.88	13.5	8.9	3.8	9.7	1.80	7.1	3.4	7.9
13.65	12.7	9.1	3.8	9.8	1.44	7.3	3.4	8.0
13.40	10.7	10	3.8	10	0.81	9.4	3.4	10

* δ_e:experimental error, δ_r:error of nuclear data ,
  $\delta_t^2=\delta_r^2+\delta_e^2$
* Error of neutron energy was estimated as about 50 keV.

Table 8(b) Activation cross section of short-lived nuclei

$^{106}Pd(n,np)^{105m}Rh$ (42.4 s)					$^{108}Pd(n,2n)^{107m}Pd$ (21.3 s)			
En(MeV)	σ(mb)	δ_e(%)	δ_r(%)	δ_t(%)	σ(mb)	δ_e(%)	δ_r(%)	δ_t(%)
14.87	1.21	25	3.8	26	472	3.6	4.8	6.0
14.58	1.40	35	3.8	35	474	3.6	4.8	6.0
14.28	0.90	42	3.8	42	455	3.7	4.8	6.0
13.88	0.47	35	3.8	36	435	3.4	4.8	5.9
13.65					473	4.3	4.8	6.4
13.40					431	3.6	4.8	6.0
$^{108}Pd(n,p)^{108g}Rh$ (6.0 min)					$^{108}Rd(n,np)^{107}Rh$ (21.7 min)			
En(MeV)	σ(mb)	δ_e(%)	δ_r(%)	δ_t(%)	σ(mb)	δ_e(%)	δ_r(%)	δ_t(%)
14.87	4.7	16	21	26	1.80	6.2	8.3	10
14.58	4.0	17	21	26	1.14	8.6	8.3	12
14.28	2.8	19	21	28	0.87	12.2	8.3	15
13.88	2.6	17	21	26	0.54	12.5	8.3	15
13.65	1.8	17	21	26	0.30	19.6	8.3	21
13.40	2.8	18	21	27	0.32	18.8	8.3	21
$^{112}Cd(n,\alpha)^{109m}Pd$ (4.69 min)					$^{116}Cd(n,p)^{116g}Ag$ (2.68 min)			
En(MeV)	σ(mb)	δ_e(%)	δ_r(%)	δ_t(%)	σ(mb)	δ_e(%)	δ_r(%)	δ_t(%)
14.87	0.61	30	3.3	30	2.30	10	6.1	12
14.58	0.59	27	3.3	27	1.69	9.8	6.1	12
14.28	0.52	23	3.3	23	1.48	11	6.1	13
13.88	0.52	19	3.3	20	1.33	10	6.1	12
13.65	0.37	28	3.3	28	0.90	13	6.1	14
13.40	0.38	25	3.3	25	0.78	13	6.1	14
$^{119}Sn(n,p)^{119g}In$(2.4 min)					$^{119}Sn(n,p)^{119m}In$(18.0 min)			
En(MeV)	σ(mb)	δ_e(%)	δ_r(%)	δ_t(%)	σ(mb)	δ_e(%)	δ_r(%)	δ_t(%)
14.87	6.25	5.3	5.1	7.4	4.69	10	20	23
14.58	5.36	6.3	5.1	8.2				
14.28	5.12	6.7	5.1	8.4				
13.88	4.08	6.3	5.1	8.1				
13.65								
13.40	3.00	7.1	5.1	8.7				

* δ_e:experimental error, δ_r:error of nuclear data, $\delta_t^2=\delta_r^2+\delta_e^2$
* Error of neutron energy was estimated as about 50 keV.

Table 8(c) Activation cross section of short-lived nuclei

	$^{120}Sn(n,p)^{120m1}In$ (43.5 s)				$^{120}Sn(n,p)^{120m2}In$ (45.6 s)			
En(MeV)	σ(mb)	δ_e(%)	δ_r(%)	δ_t(%)	σ(mb)	δ_e(%)	δ_r(%)	δ_t(%)
14.87	4.8	12	11	16	0.95	19	5.1	20
14.58	4.0	16	11	18	0.85	29	5.1	24
14.28	3.4	17	11	20	0.59	34	5.1	34
13.88	2.6	17	11	20	0.48	32	5.1	32
13.65	2.8	16	11	19	0.46	32	5.1	32
13.40	1.9	18	11	20	0.43	32	5.1	32

* δ_e:experimental error, δ_r:error of nuclear data, $\delta_t^2=\delta_r^2+\delta_e^2$
* Error of neutron energy was estimated as about 50 keV.

Table 9 Results of half-life measurement

Nuclide	Production reaction	E_γ (keV)	Reference[a] (E_γ in keV)	Half-life Present	Reference
^{105m}Rh	$^{105}Pd(n,p)$	129.6	^{170}Tm (84.3)	42.4(5) s	45 s[b]
$^{120m1}In$	$^{120}Sn(n,p)$	863.3	^{137}Cs (661.7)	43.5(8) s	46.2(8) s[c]
$^{120m2}In$	$^{120}Sn(n,p)$	197.3	^{241}Am (59.5)	45.6(7) s	47.3(5) s[c]

a) These sources were used for corrections of dead-time and pile-up losses.
b) Taken from ref. 10.
c) Taken from ref. 17.

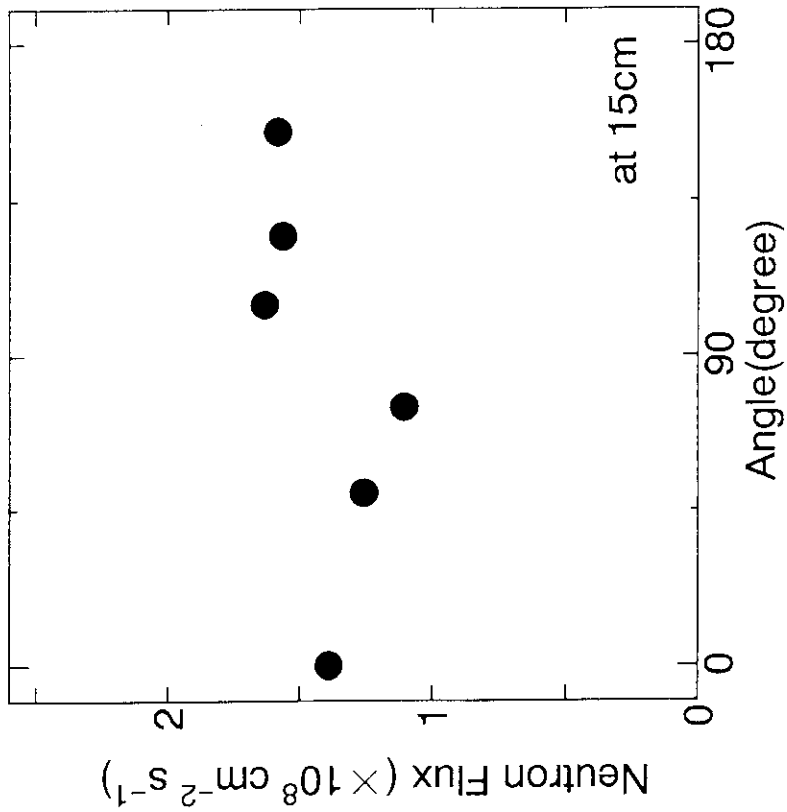

Fig. 2 Neutron flux at 15 cm.

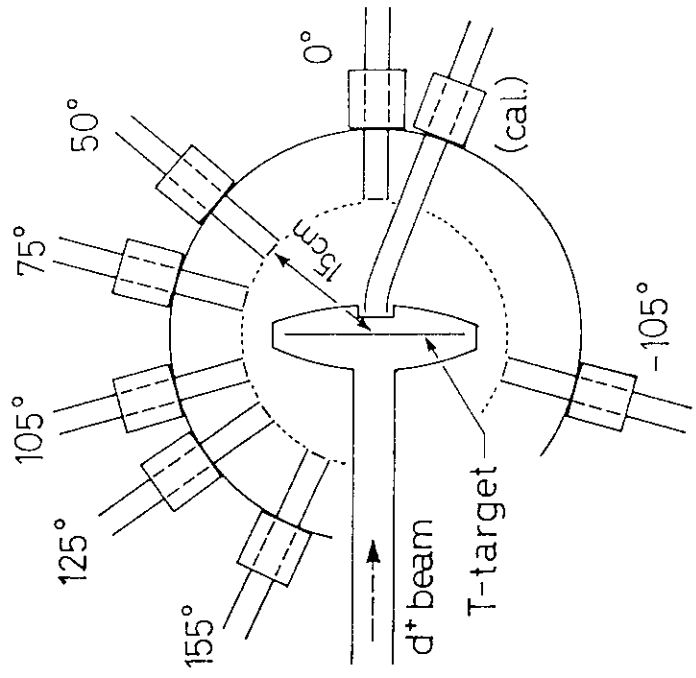

Fig. 1 Pneumatic sample transport system at OKTAVIAN. The distance between T-target and the irradiation position was 15 cm. The additional tube is set at −22.5° and 1.5 cm. The neutron flux at 1.5 cm is 50 times as high as at 15 cm.

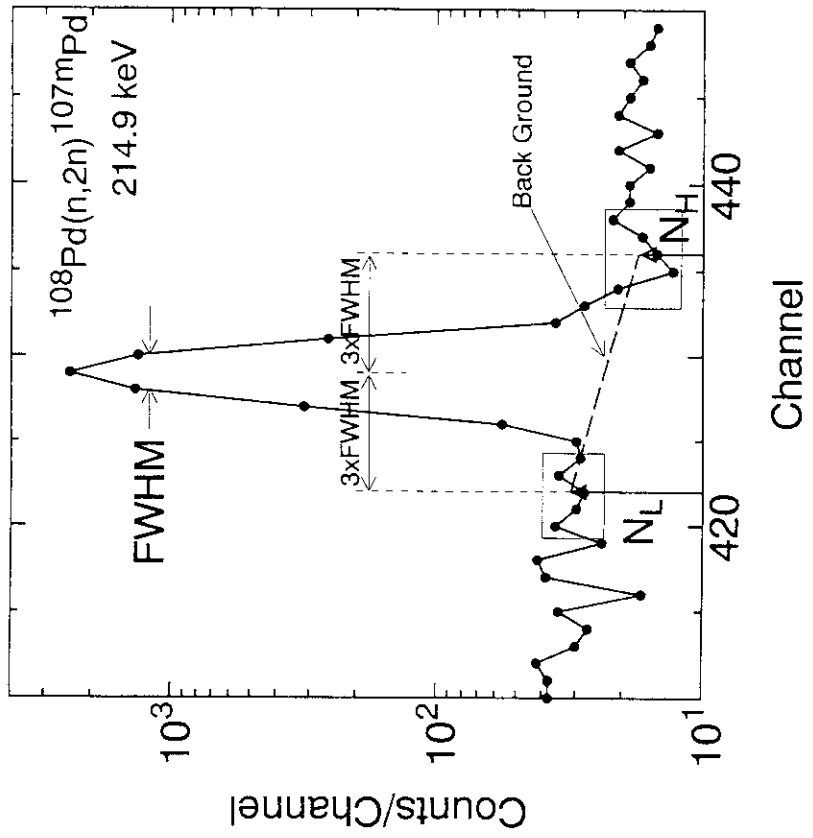

Fig. 4 Peak area evaluation of 214.9 keV γ-ray in the decay of ^{107m}Pd.

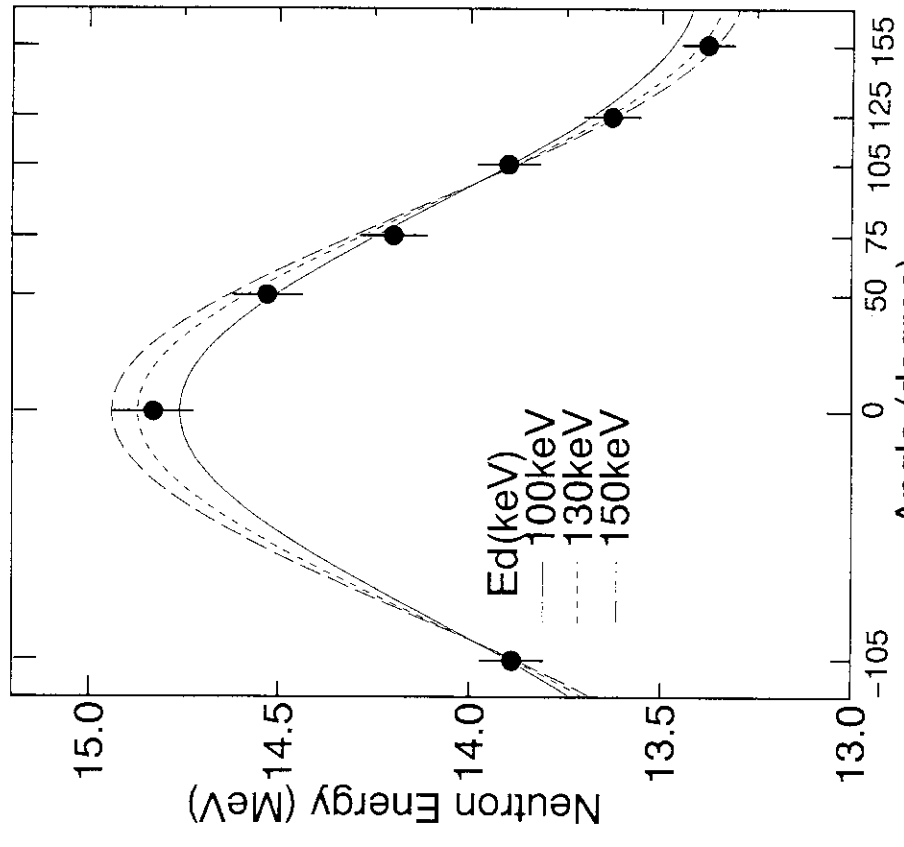

Fig. 3 Angular dependences of d-T neutron energy. The best fitting value of E_d (effective d^+ energy) is 130 keV.

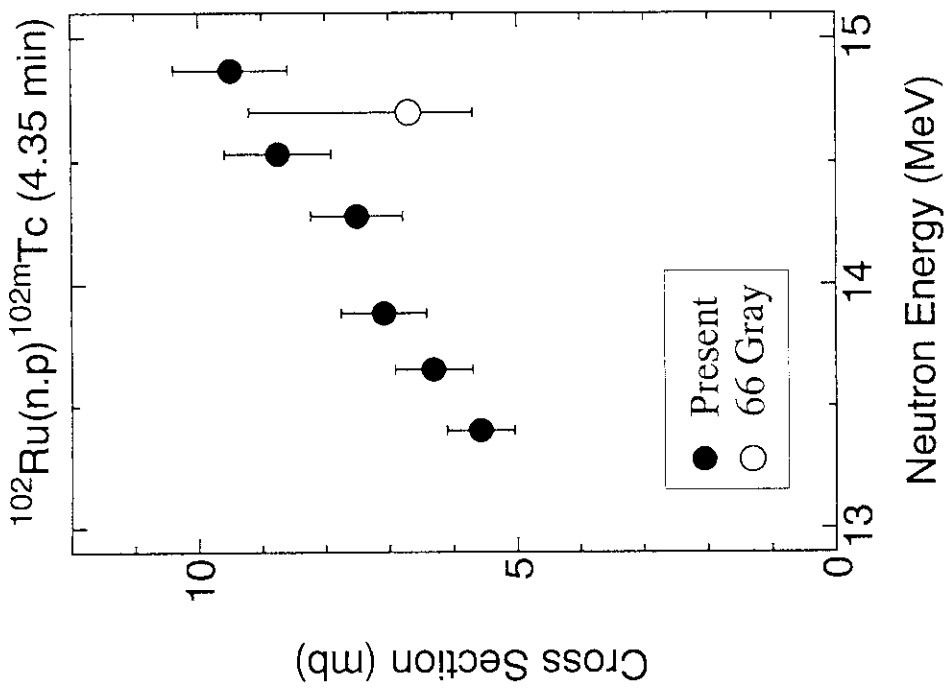

Fig. 5.2 Cross section of ^{102}Ru(n,p)^{102m}Tc.

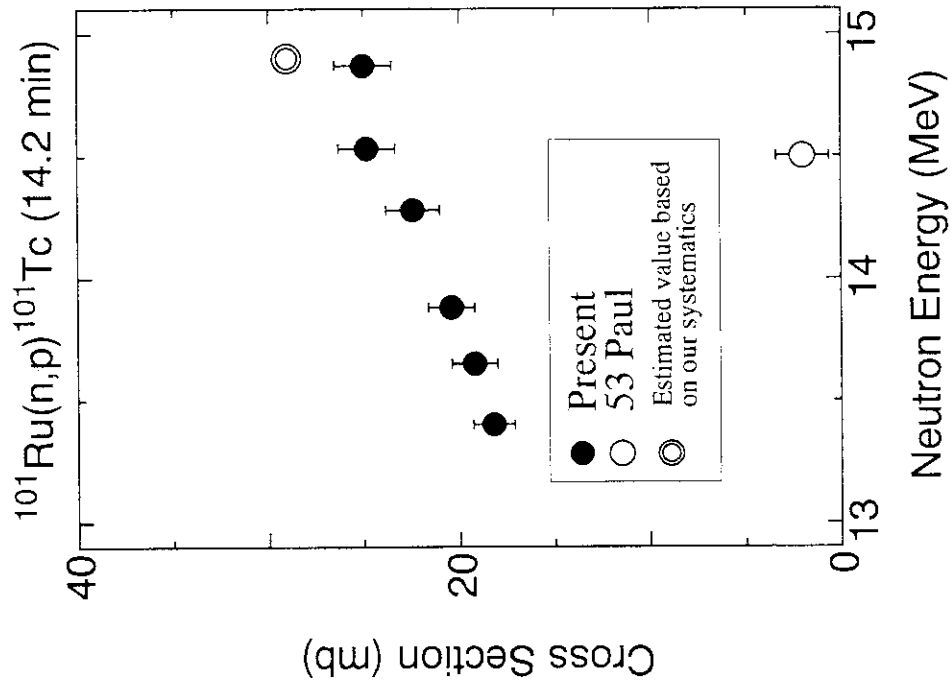

Fig. 5.1 Cross section of ^{101}Ru(n,p)^{101}Tc. The double circle shows an estimated value based on our systematics.

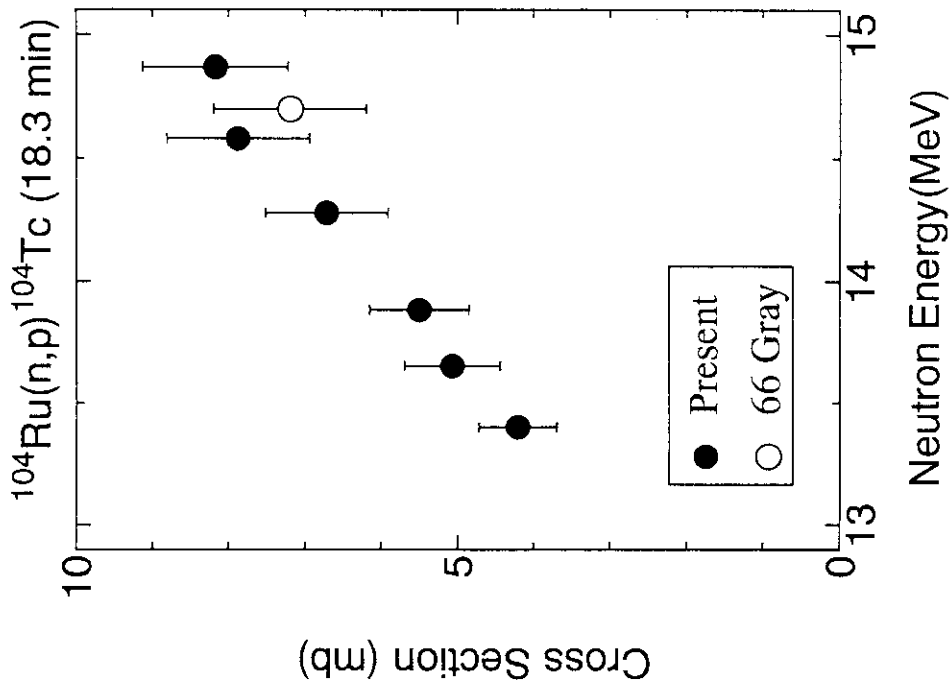

Fig. 5.4 Cross section of ^{104}Ru(n,p)^{104}Tc.

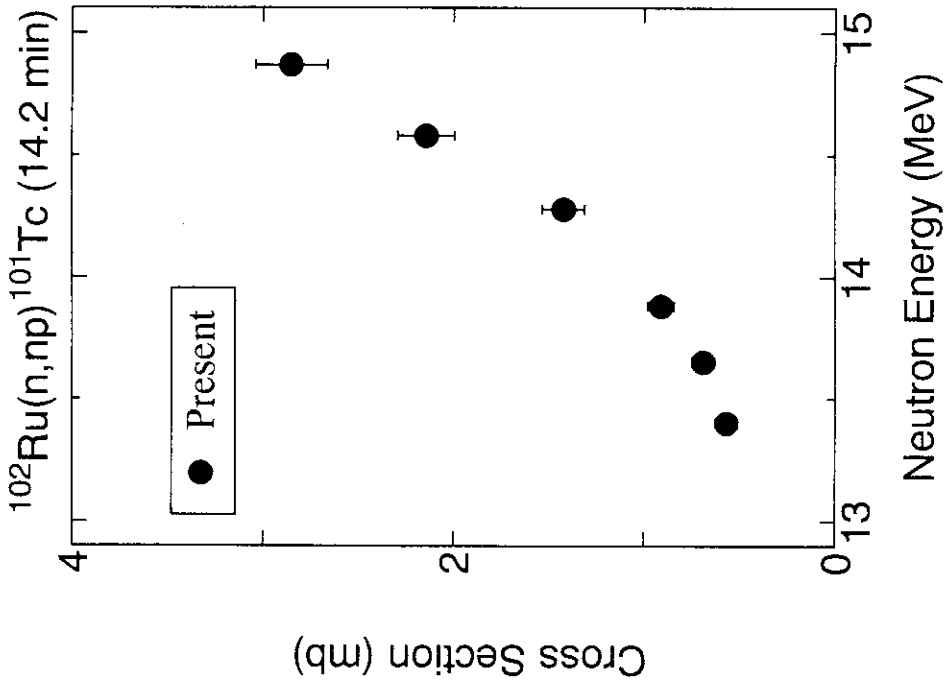

Fig. 5.3 Cross section of ^{102}Ru(n,np)^{101}Tc.

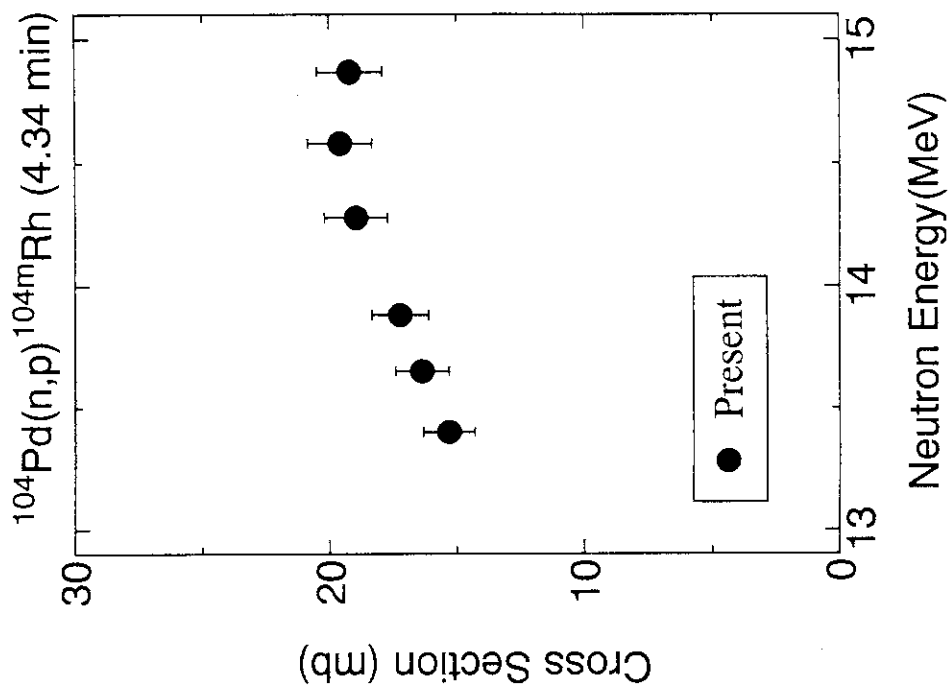

Fig. 5.6 Cross section of ^{104}Pd(n,p)^{104m}Rh.

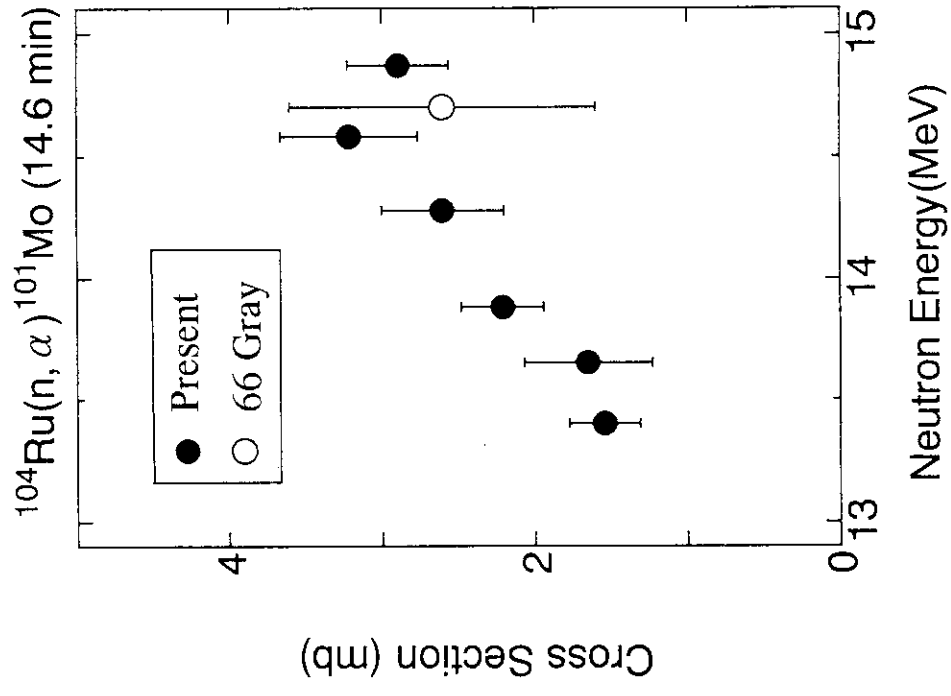

Fig. 5.5 Cross section of ^{104}Ru(n,α)^{101}Mo.

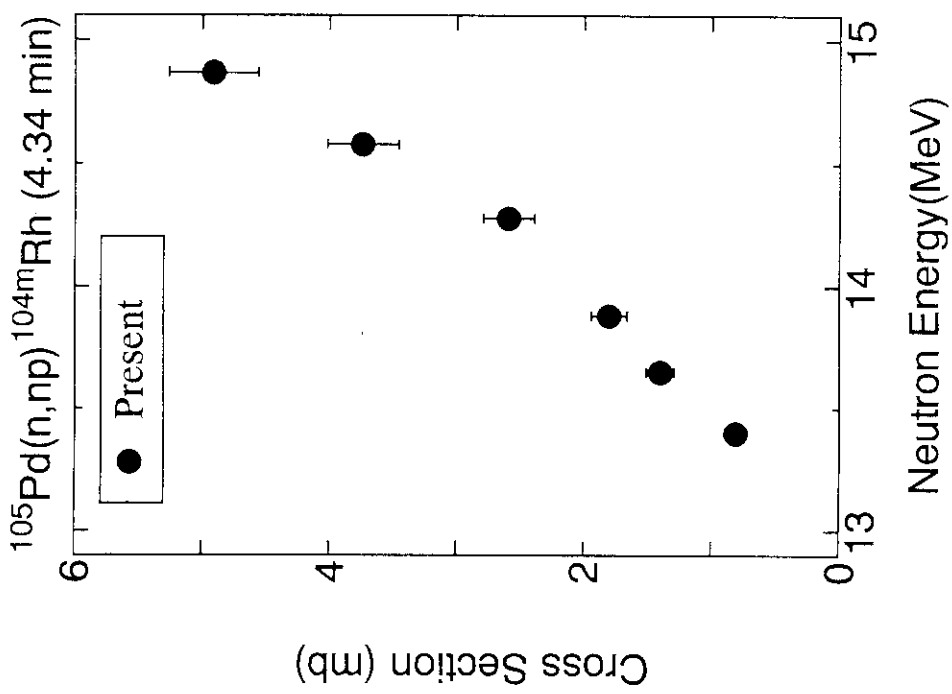

Fig. 5.8 Cross section of ^{105}Pd(n,np)^{104m}Rh.

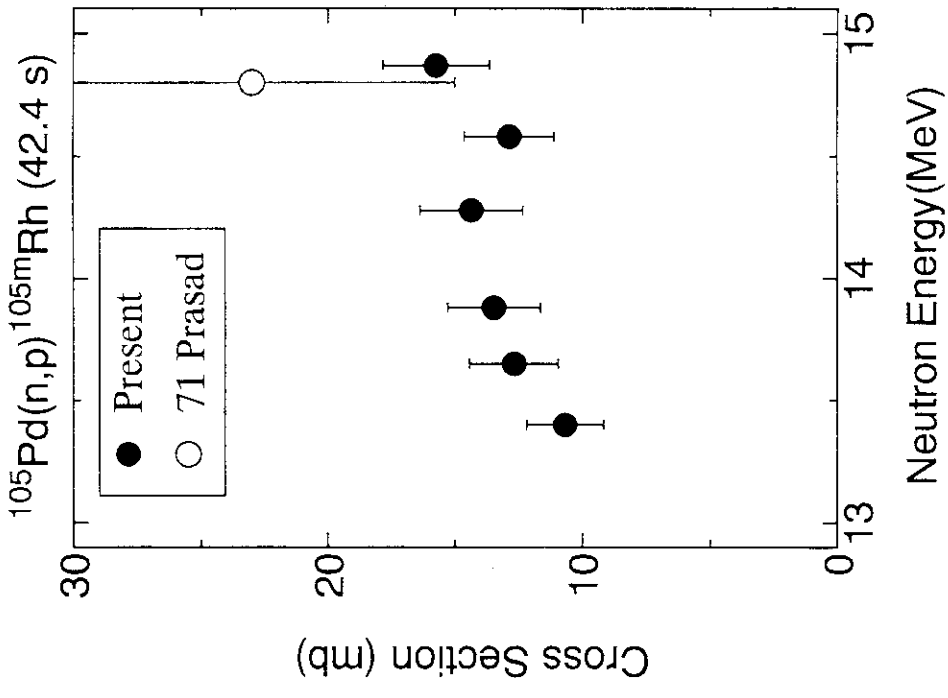

Fig. 5.7 Cross section of ^{105}Pd(n,p)^{105m}Rh.

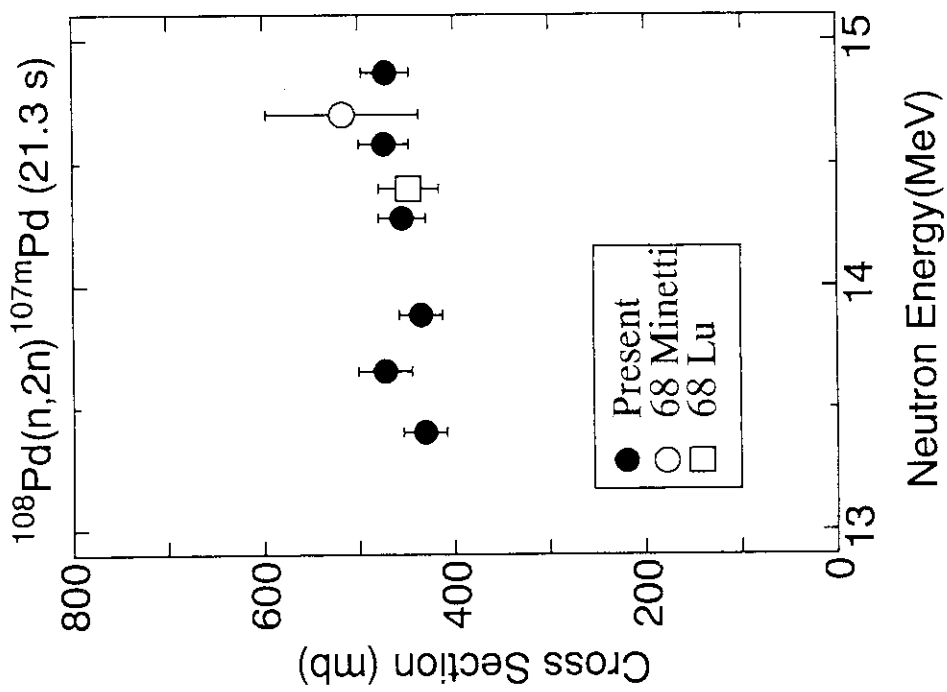

Fig. 5.10 Cross section of ^{108}Pd(n,2n)^{107m}Pd.

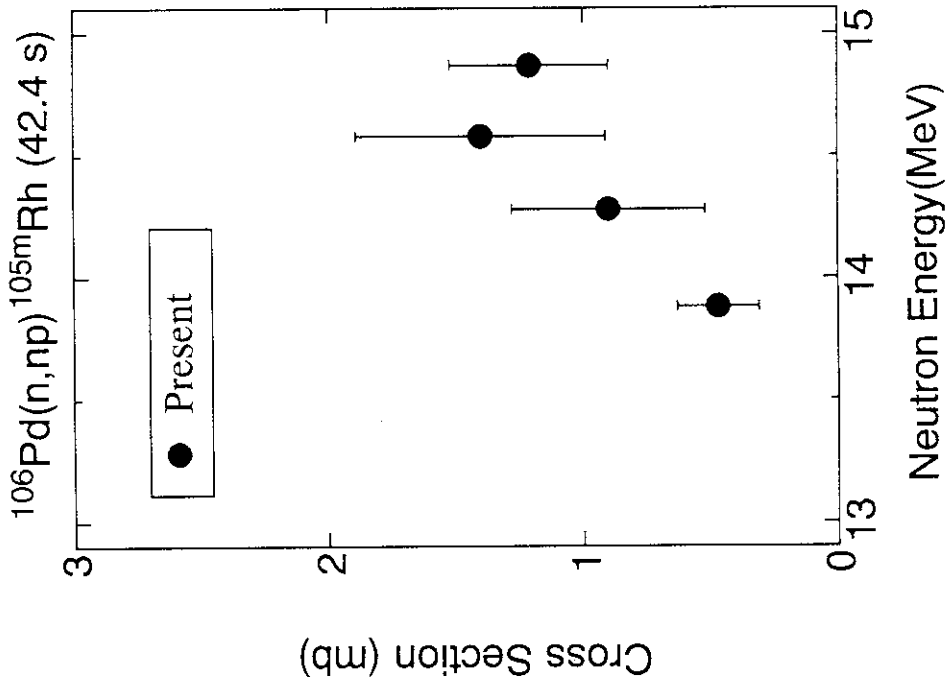

Fig. 5.9 Cross section of ^{106}Pd(n,np)^{105m}Rh.

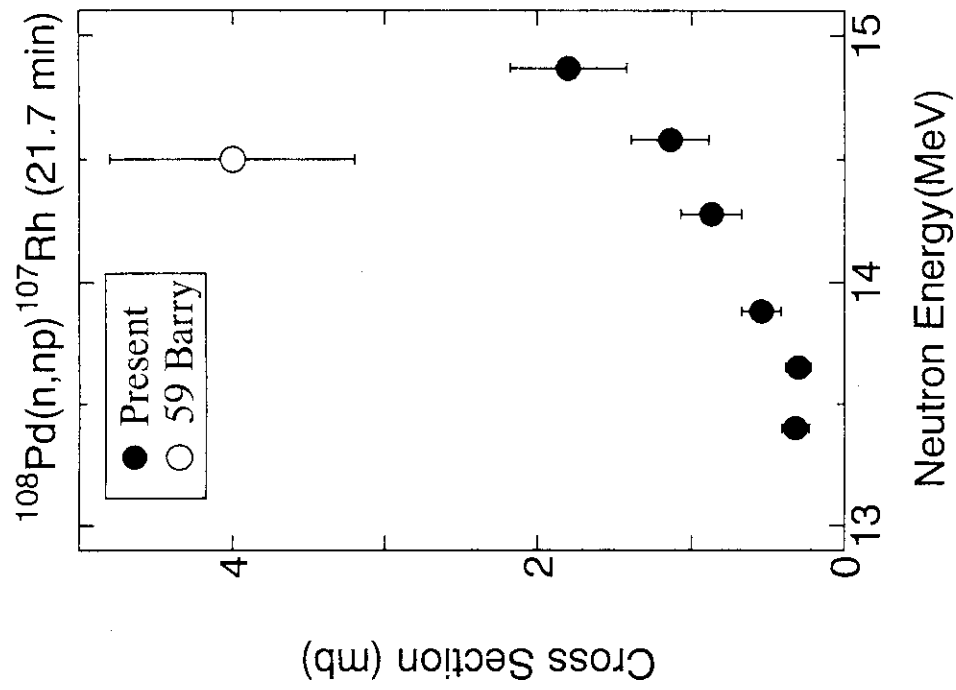

Fig. 5.12 Cross section of ^{108}Pd(n,np)^{107}Rh.

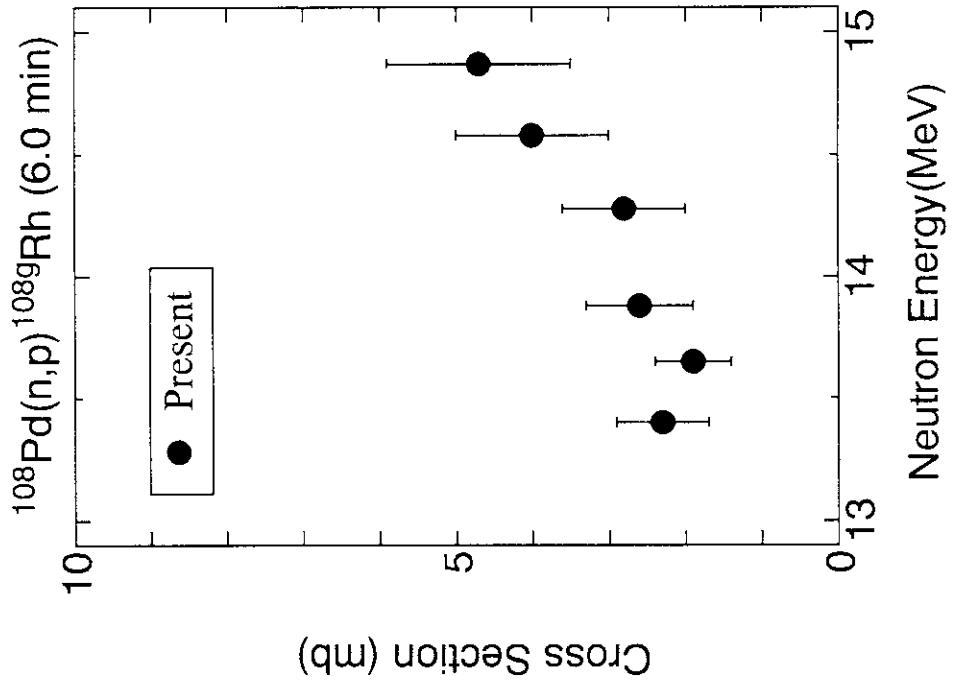

Fig. 5.11 Cross section of ^{108}Pd(n,p)^{108g}Rh.

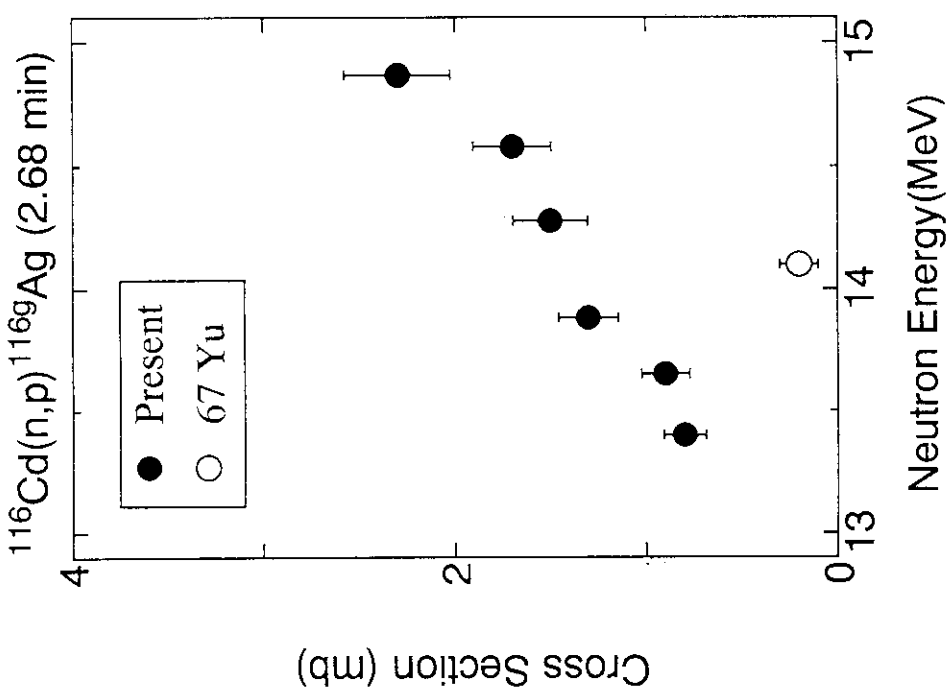

Fig. 5.14 Cross section of ^{116}Cd(n,p)^{116g}Ag.

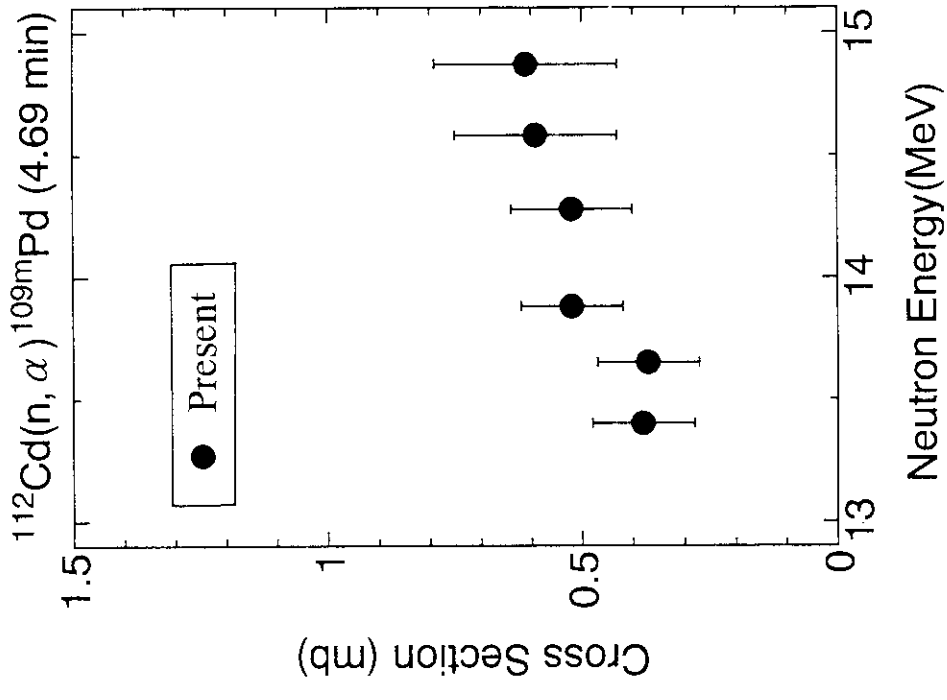

Fig. 5.13 Cross section of ^{112}Cd(n,α)^{109m}Pd.

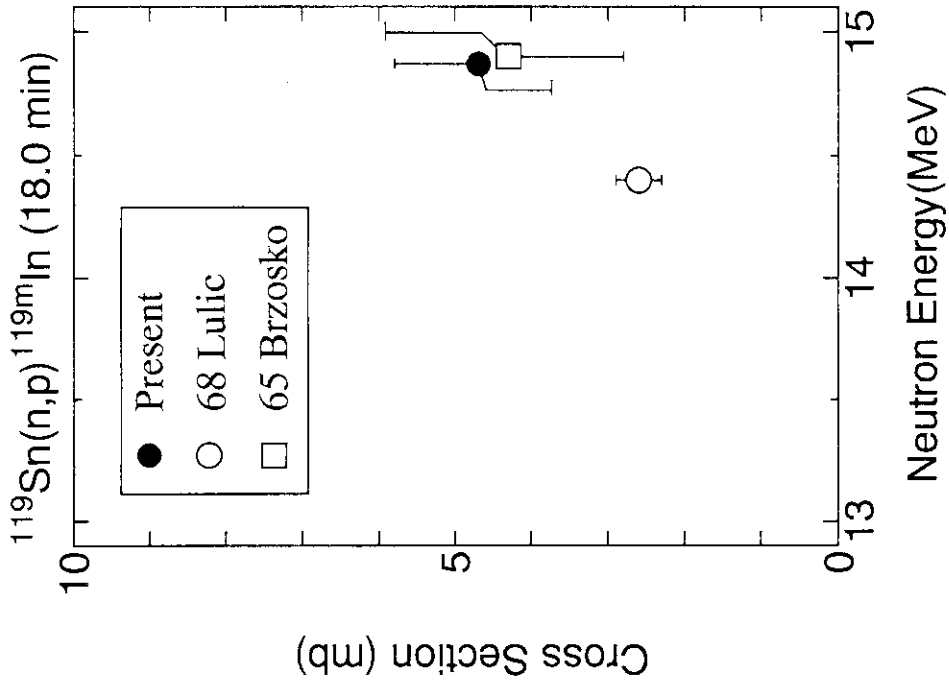

Fig. 5.16 Cross section of ^{119}Sn(n,p)^{119m}In.

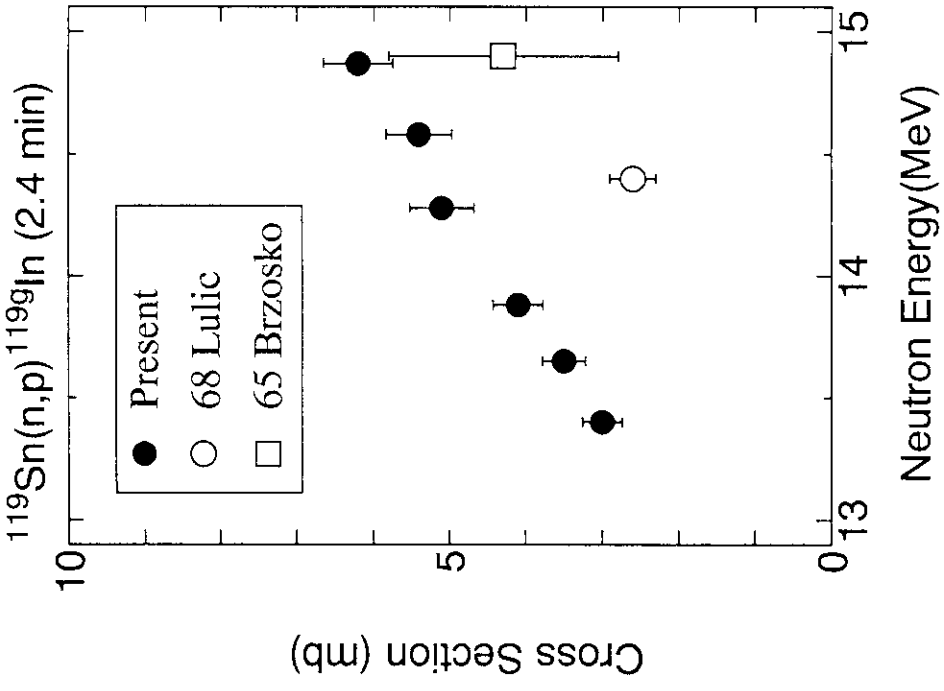

Fig. 5.15 Cross section of ^{119}Sn(n,p)^{119g}In.

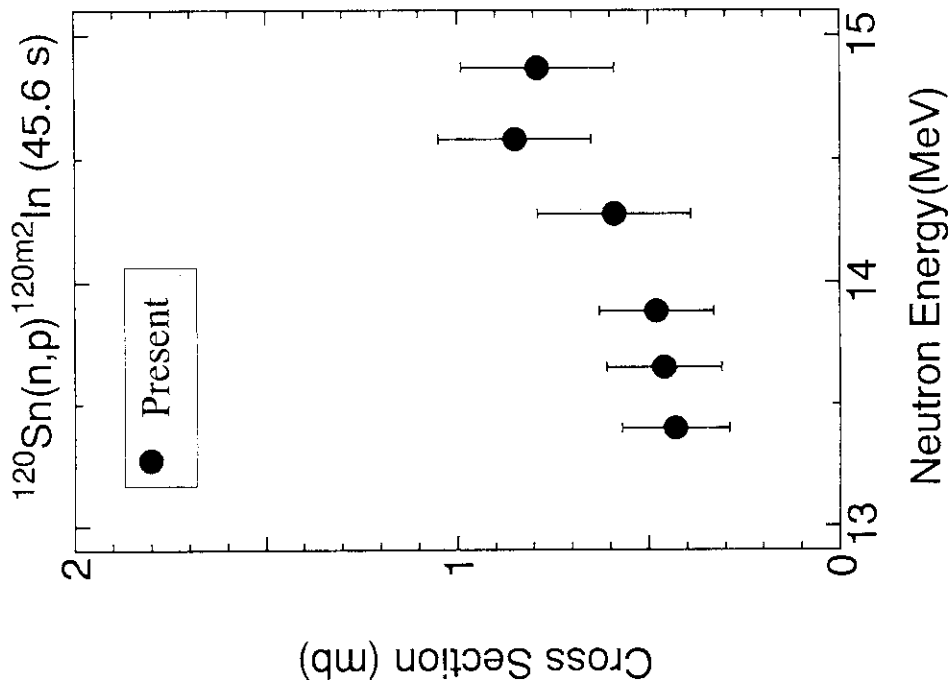

Fig. 5.18 Cross section of ^{120}Sn(n,p)^{120m2}In.

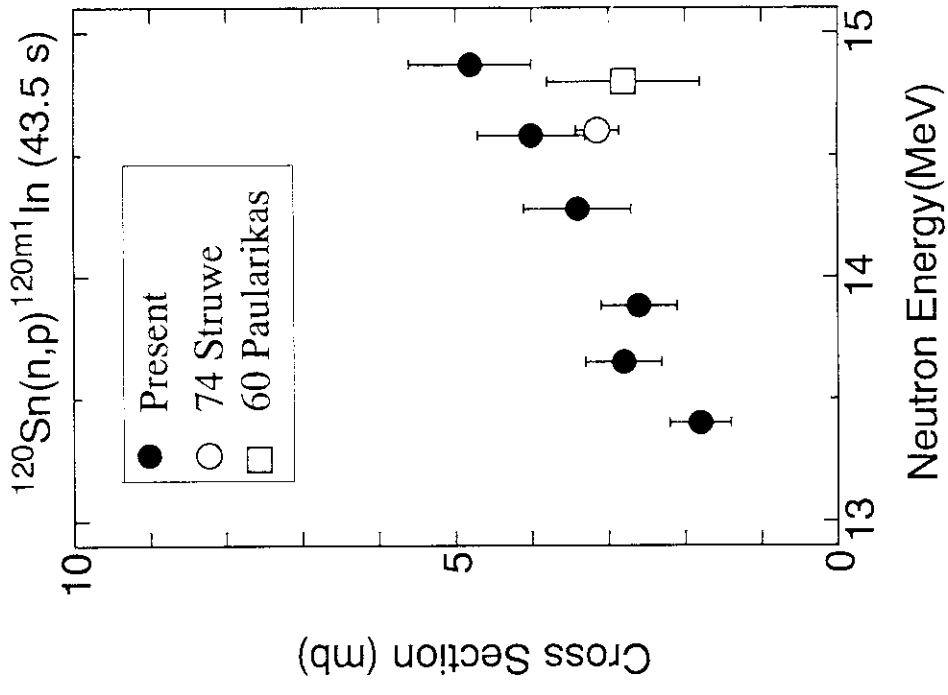

Fig. 5.17 Cross section of ^{120}Sn(n,p)^{120m1}In.

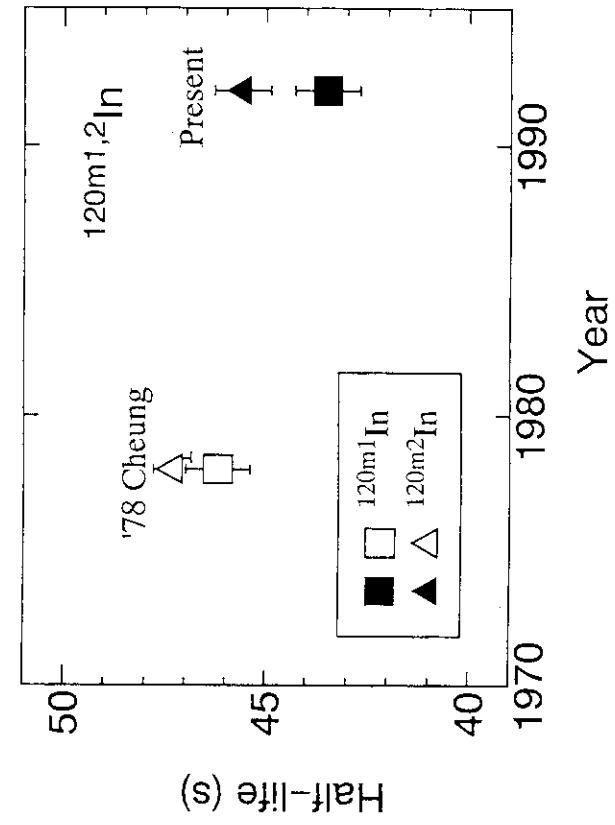

Fig. 6.2 Half-life of ^{120m}In. Squares show the half-lives of ^{120m1}In with 3^+, 4^+ or 5^+, and triangles show those of ^{120m2}In with 8^-.

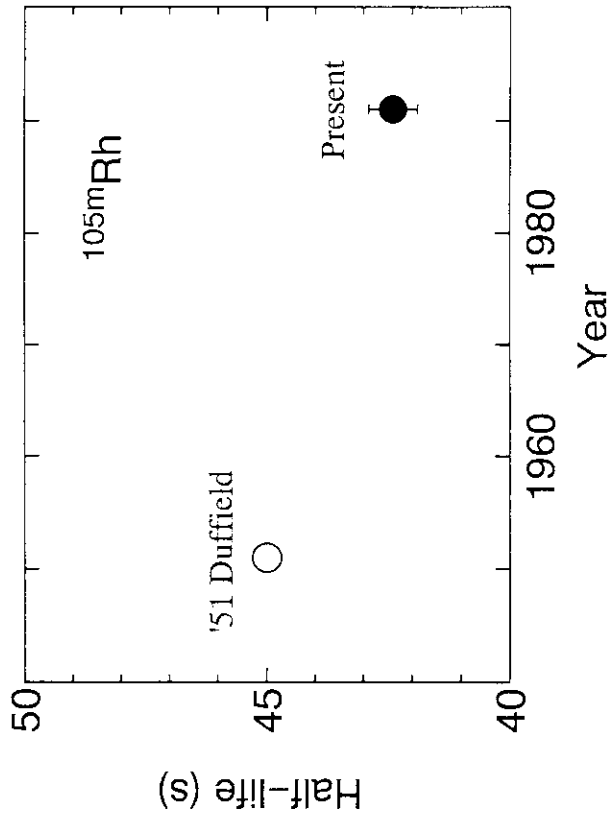

Fig. 6.1 Half-life of ^{105m}Rh.

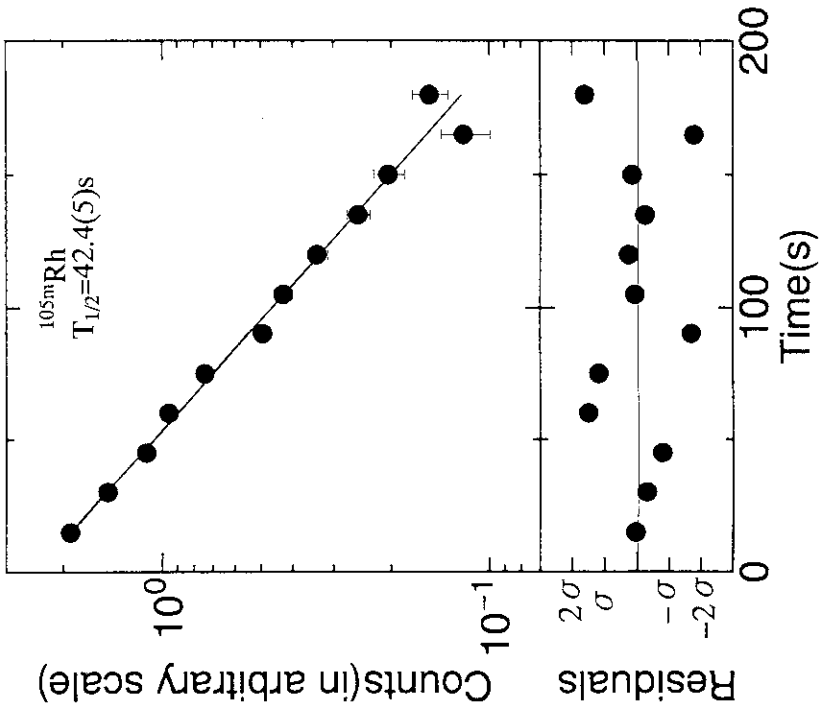

Fig. 8 Decay curve of ^{105m}Rh and residuals obtained from the least squares fitting analysis.

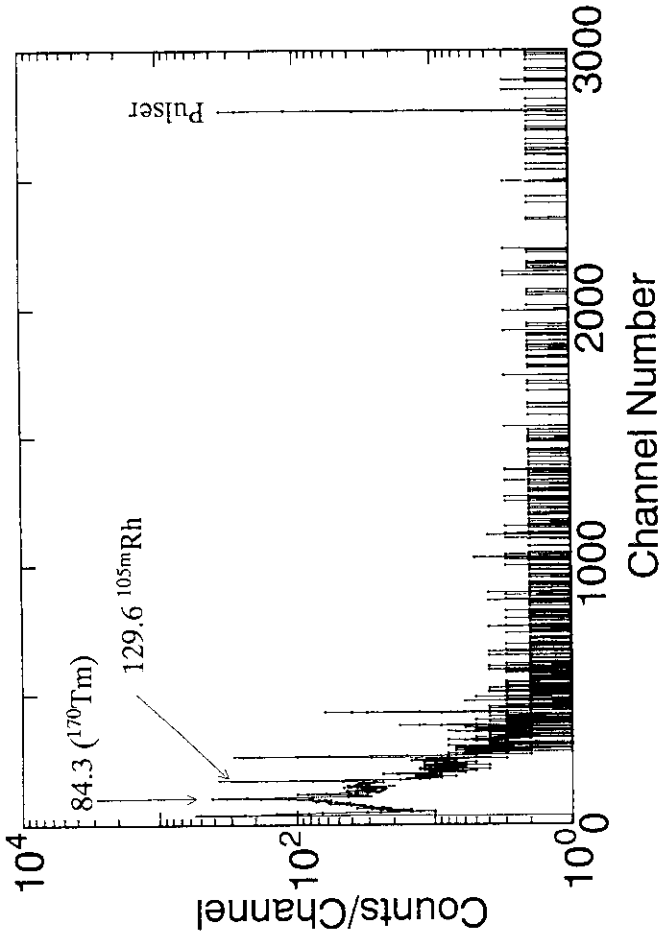

Fig. 7 Gamma-ray spectrum in the decay of ^{105m}Rh. Gamma-rays from ^{170}Tm and the pulser were simultaneously measured for the correction of pile-up losses.

Appendix 1 Gamma−ray spectra of sample irradiated by 14.9 MeV neutrons

Gamma−ray spectra of sample irradiated by 14.9 MeV neutrons are given in Fig.A.1.1 − 22. The legend which appears in the figures is explained below.

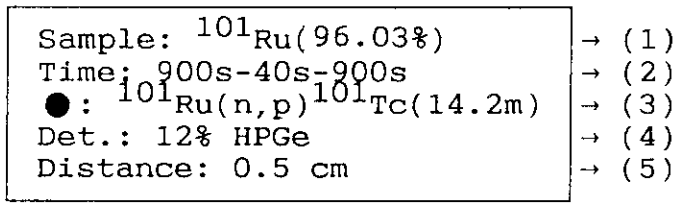

(1) Sample (enrichment % for separated isotopes)
(2) Irradiation time, cooling time, measurement time
(3) Reaction
(4) Detector. Usually Ge detectors are covered with 5mm acrylic absorber.
(5) Source−to−detector distance.

* Gamma−ray energies are given in keV. 511γ ; 511 keV annihilation γ−ray.

Irradiated samples	Fig.A.1.X X	Irradiated samples	Fig.A.1.X
^{101}Ru(96.03%);	1, 2	^{108}Pd(98.79%) ;	13, 14
^{102}Ru(98.95%);	3, 4	^{112}CdO(97.26%) ;	15, 16
^{104}Ru(99.05%);	5, 6	^{116}CdO(94.97%) ;	17, 18
^{104}Pd(96.02%);	7, 8	$^{119}SnO_2$(84.48%);	19, 20
^{105}Pd(96.58%);	9, 10	$^{120}SnO_2$(98.05%);	21, 22
^{106}Pd(97.51%);	11, 12		

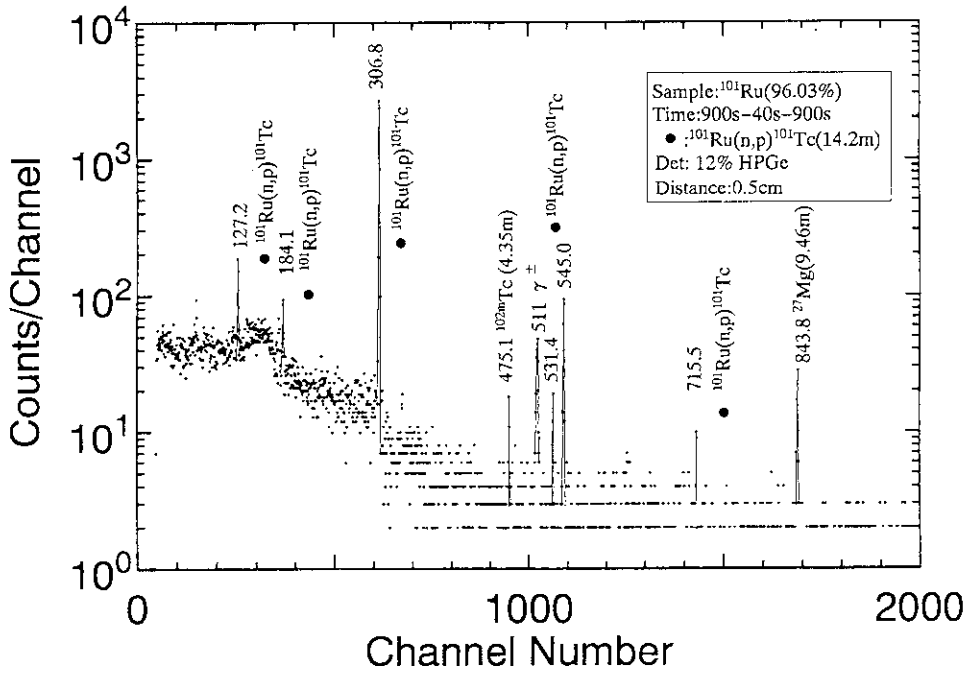

Fig. A.1.1

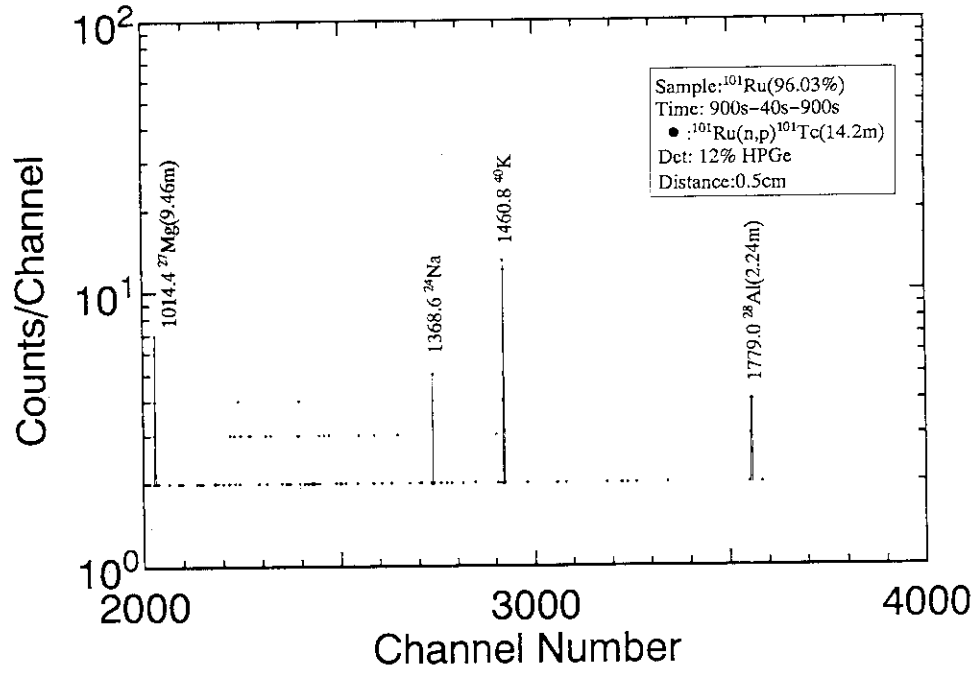

Fig. A.1.2

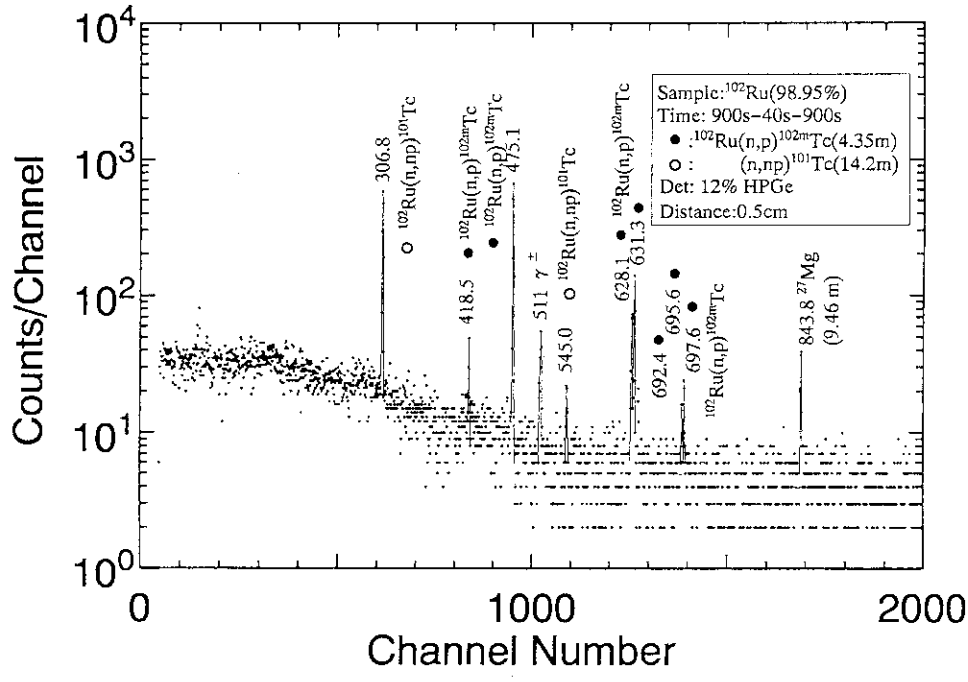

Fig. A.1.3

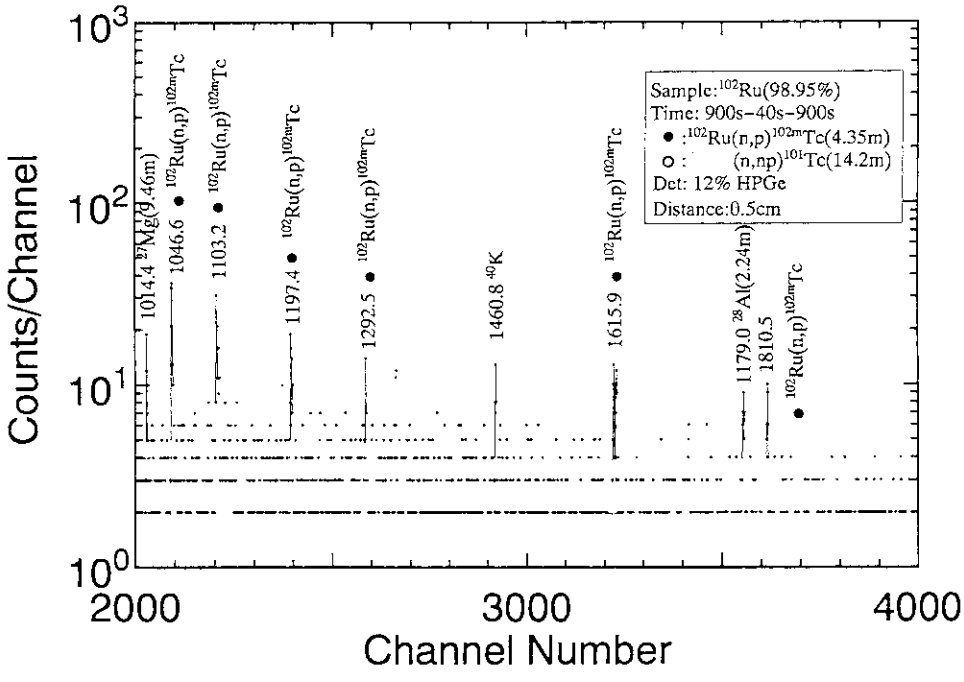

Fig. A.1.4

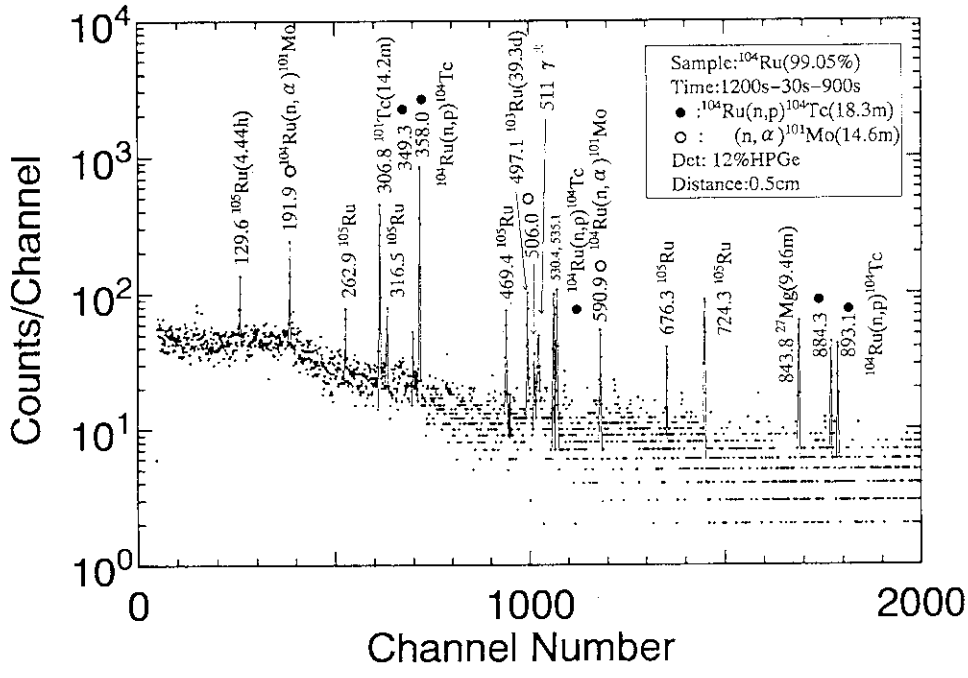

Fig. A.1.5

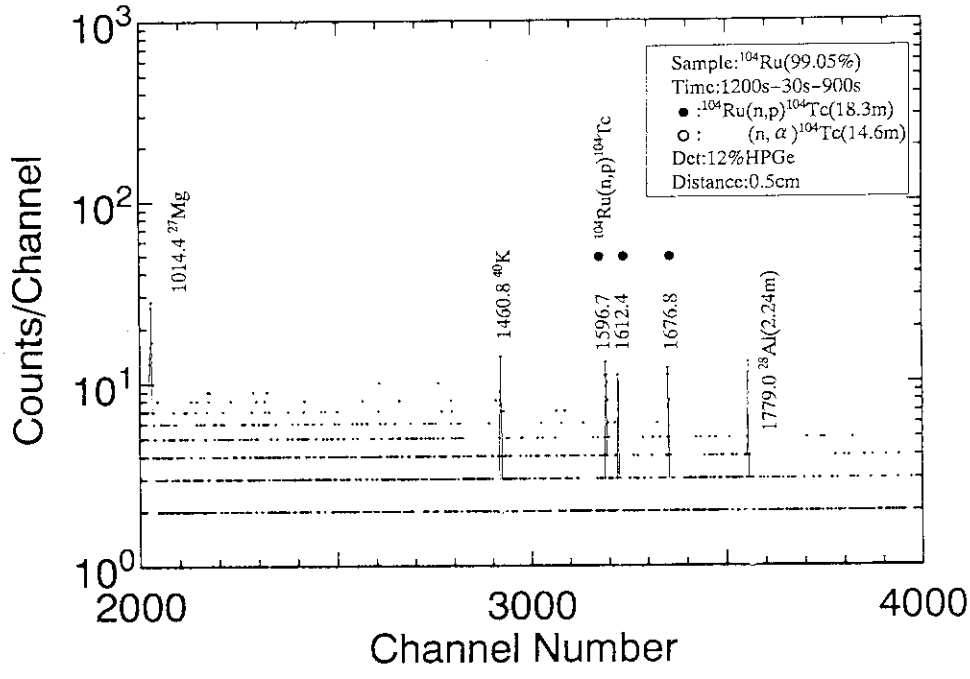

Fig. A.1.6

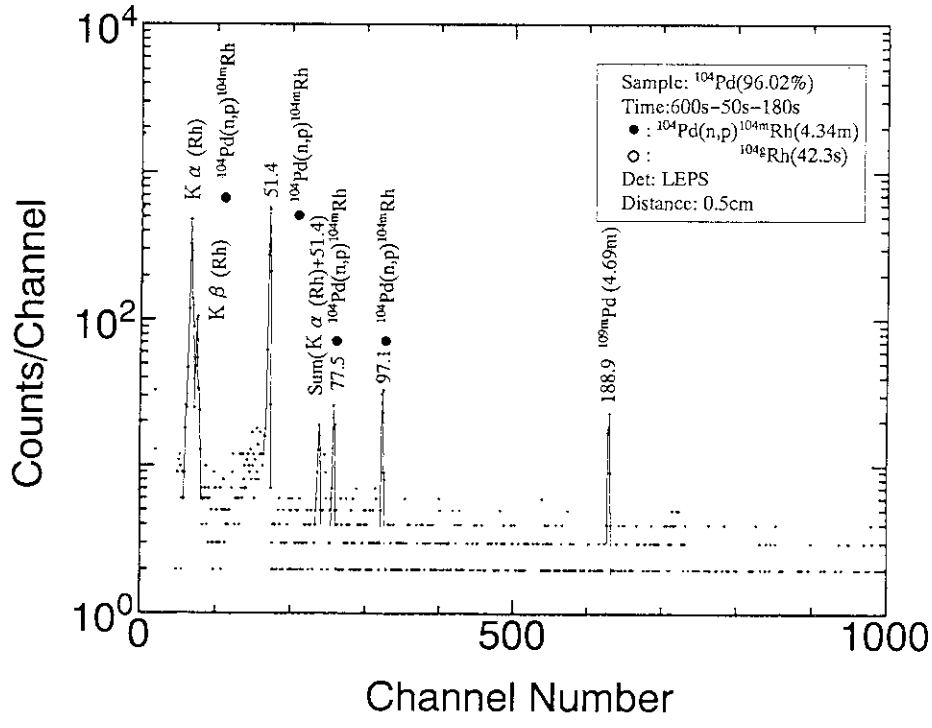

Fig. A.1.7

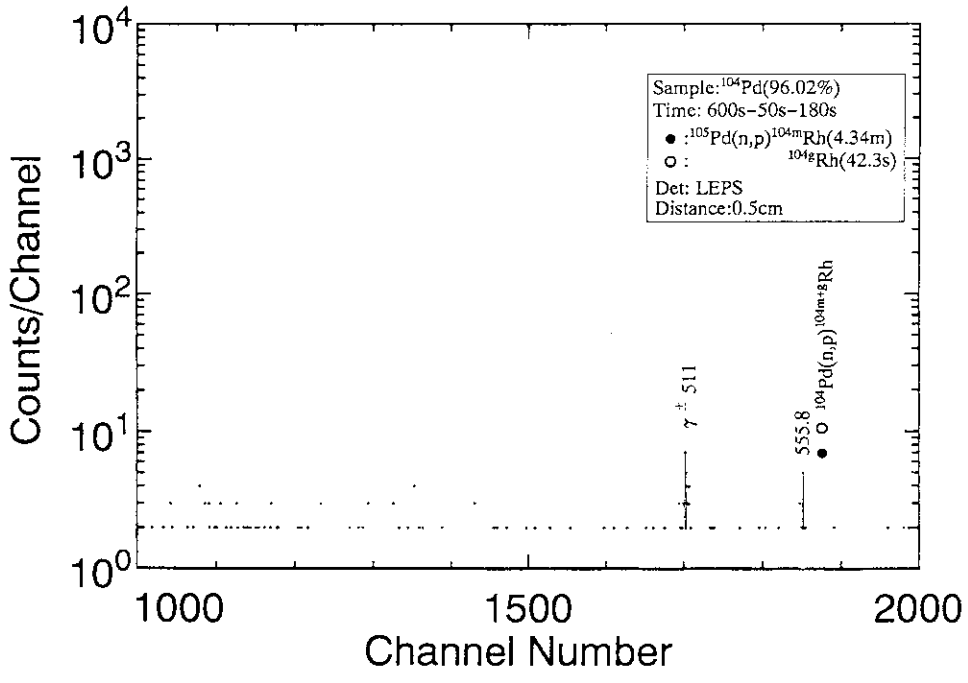

Fig. A.1.8

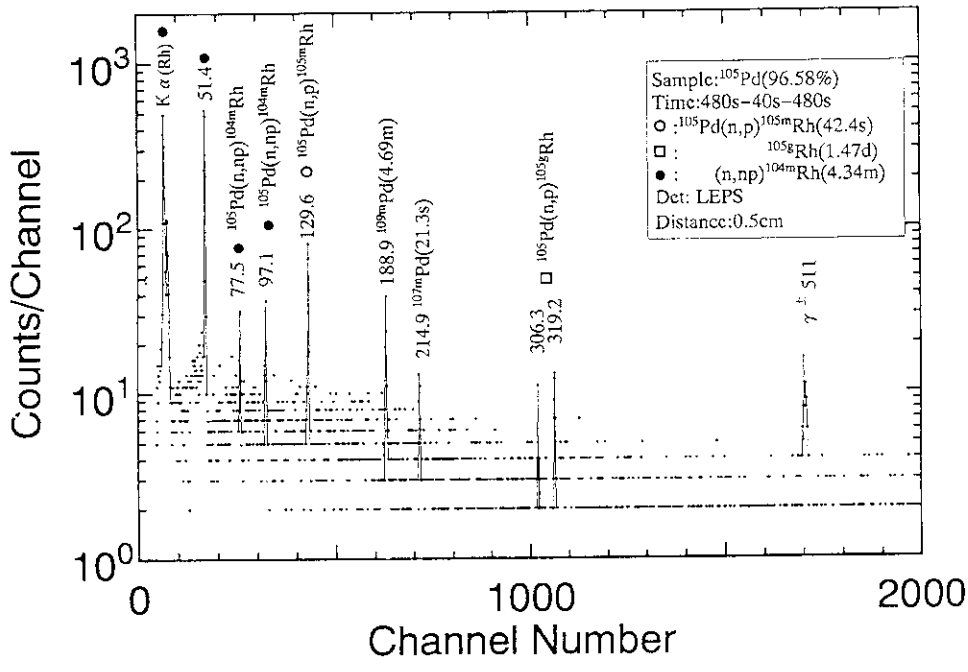

Fig. A.1.9

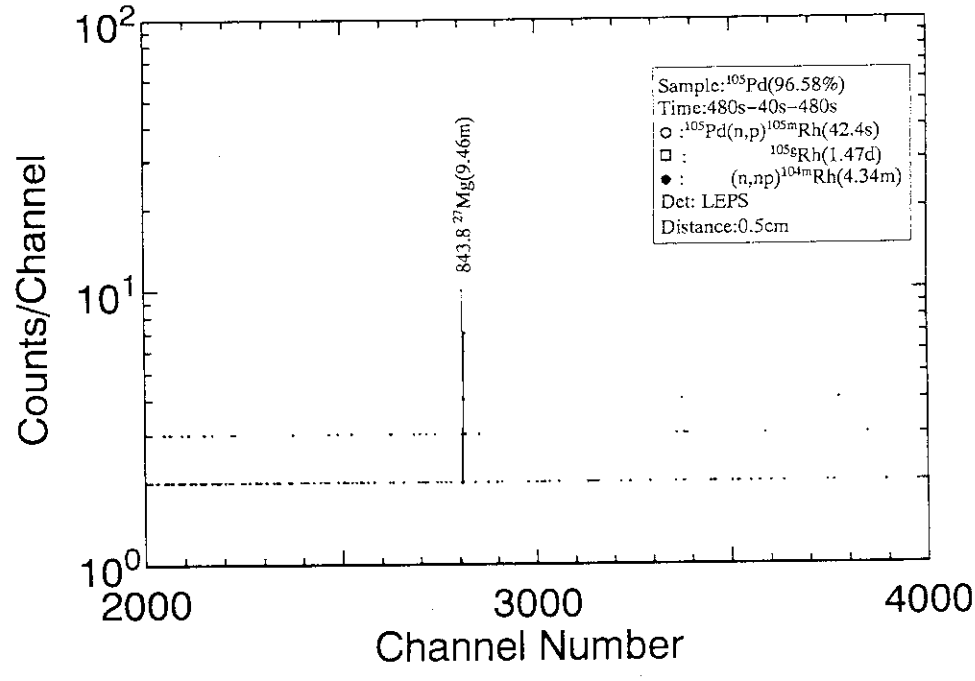

Fig. A.1.10

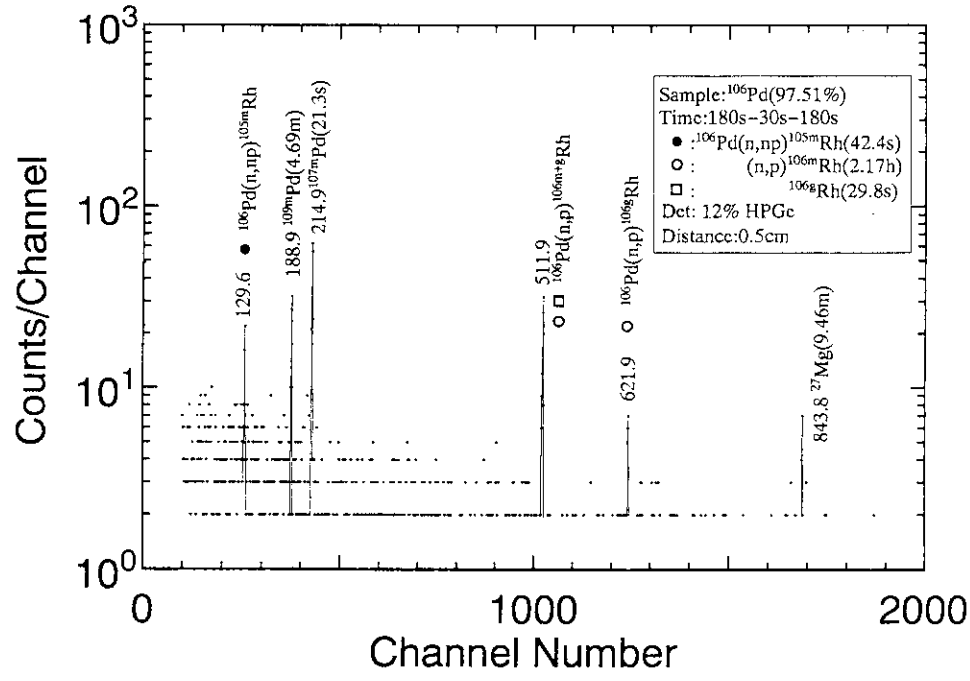

Fig. A.1.11

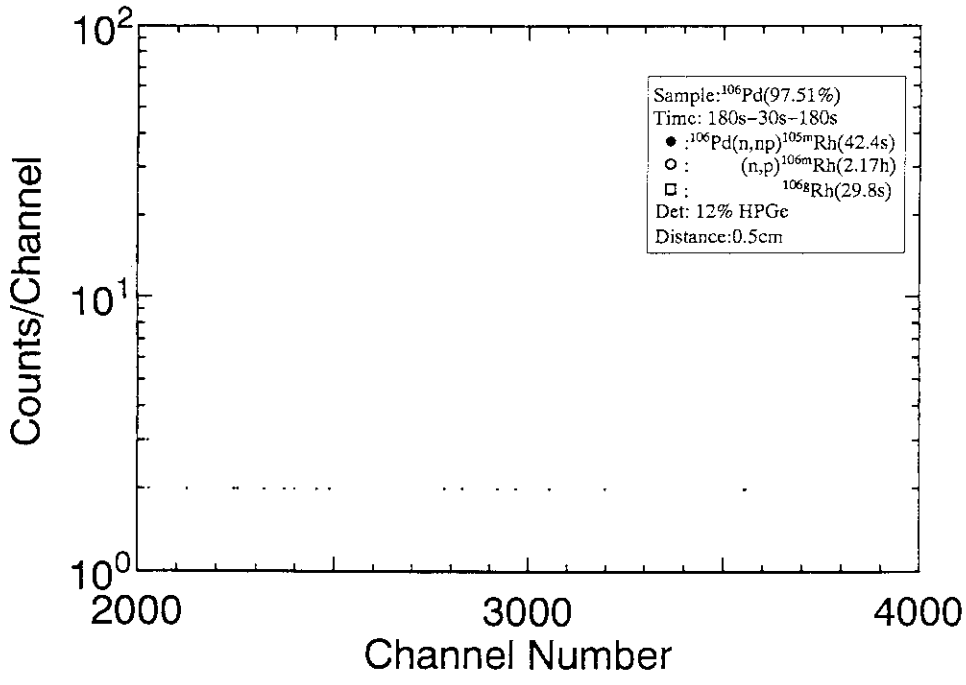

Fig. A.1.12

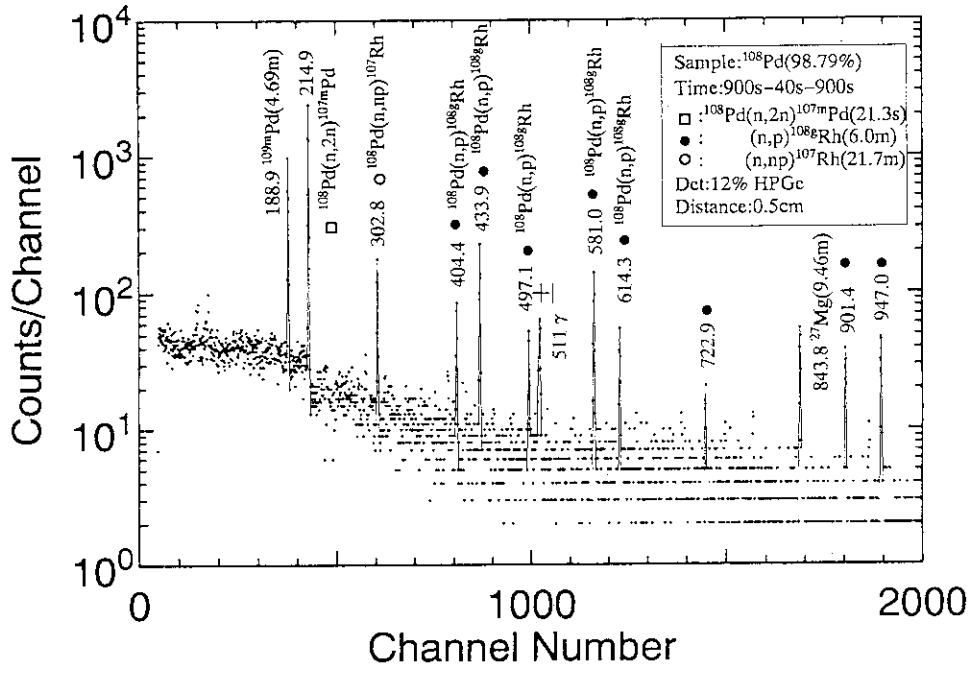

Fig. A.1.13

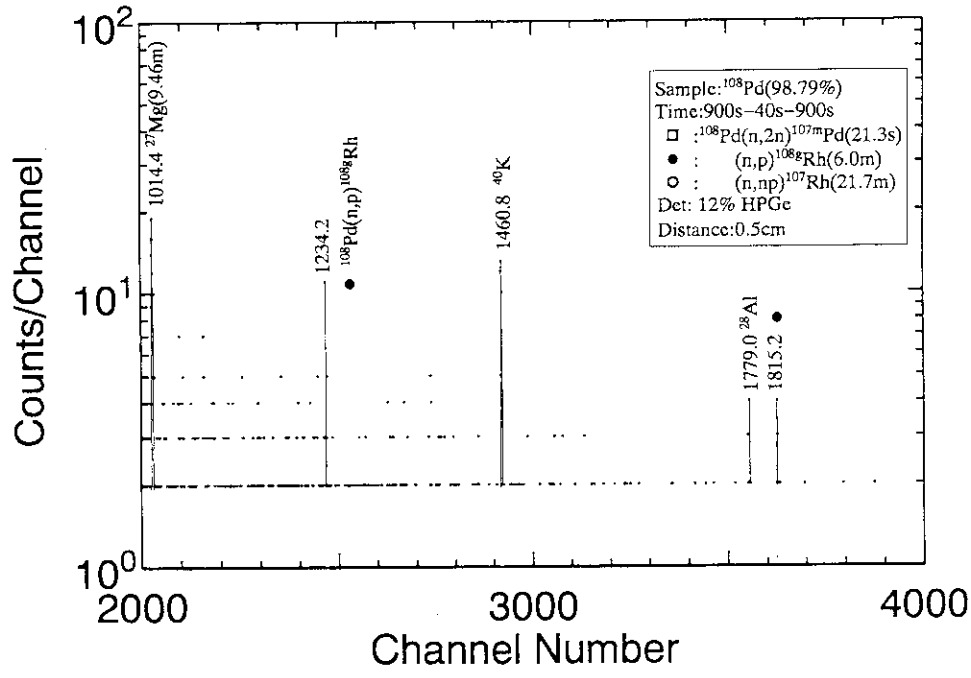

Fig. A.1.14

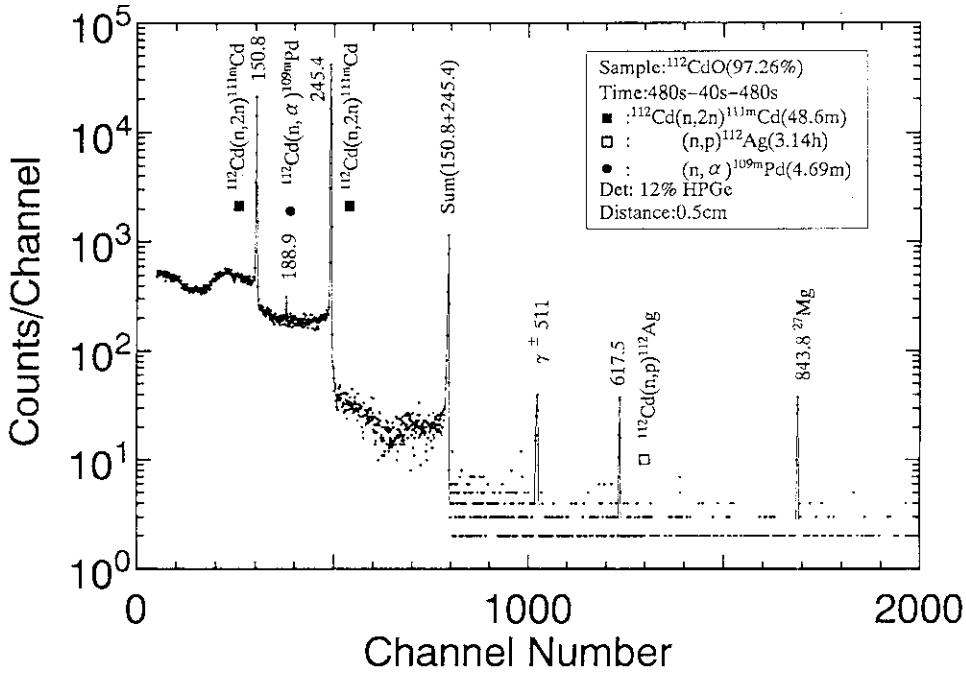

Fig. A.1.15

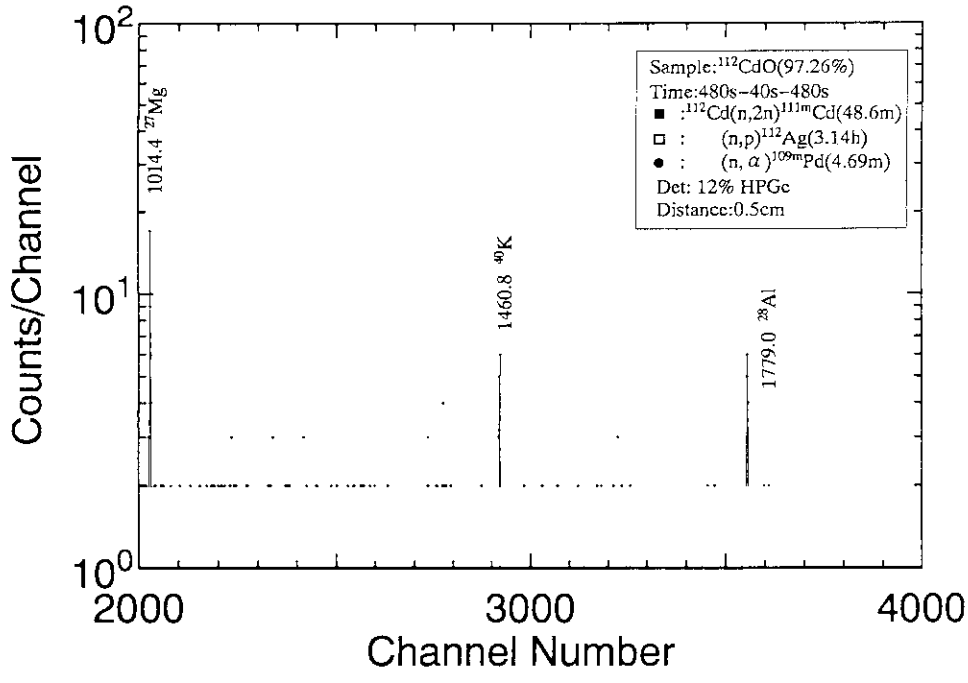

Fig. A.1.16

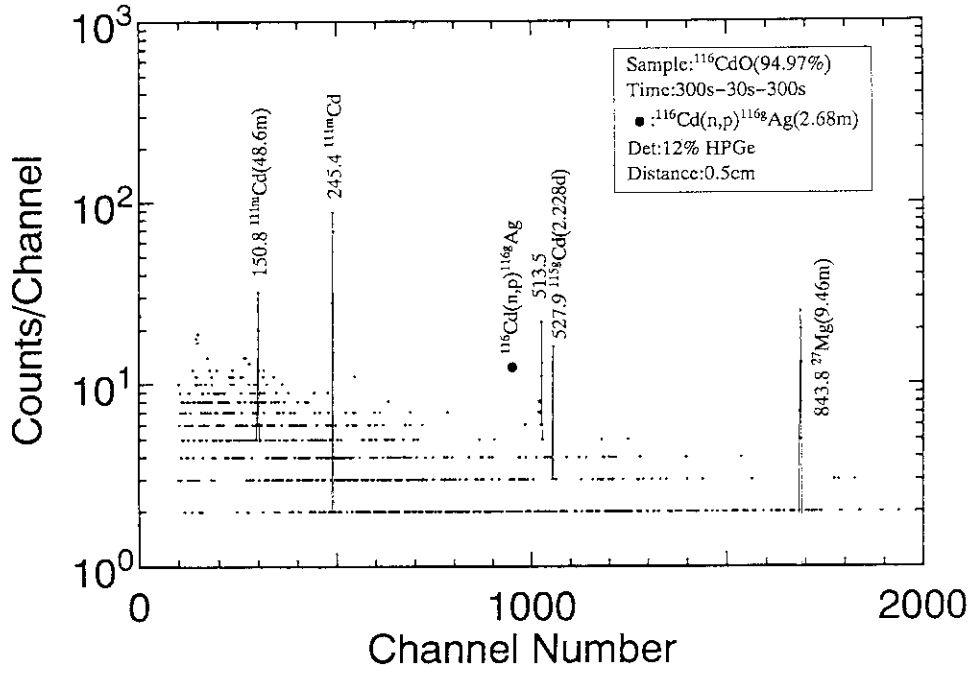

Fig. A.1.17

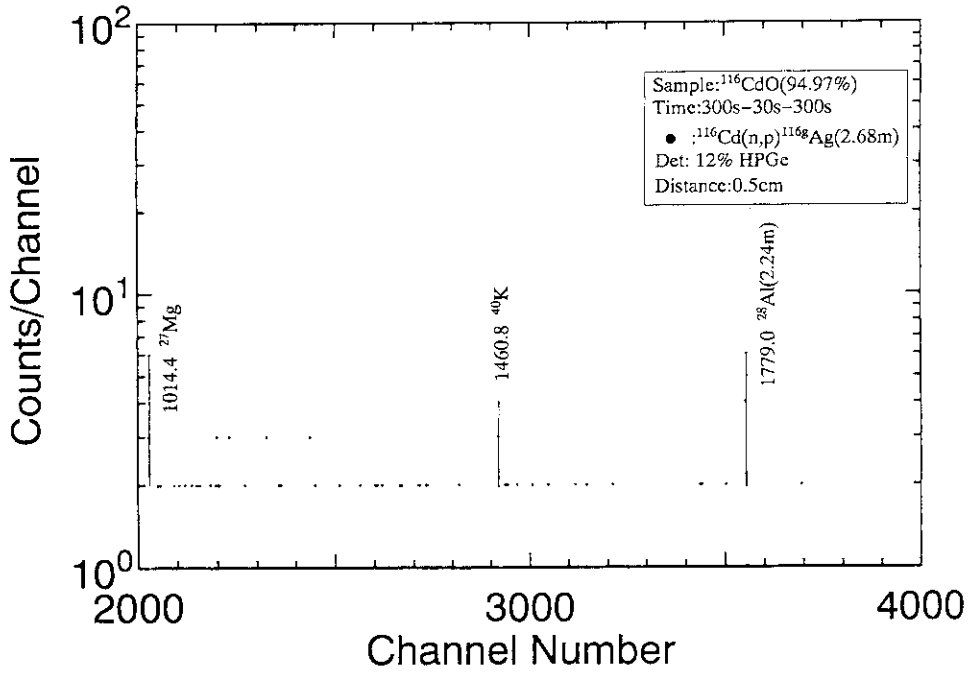

Fig. A.1.18

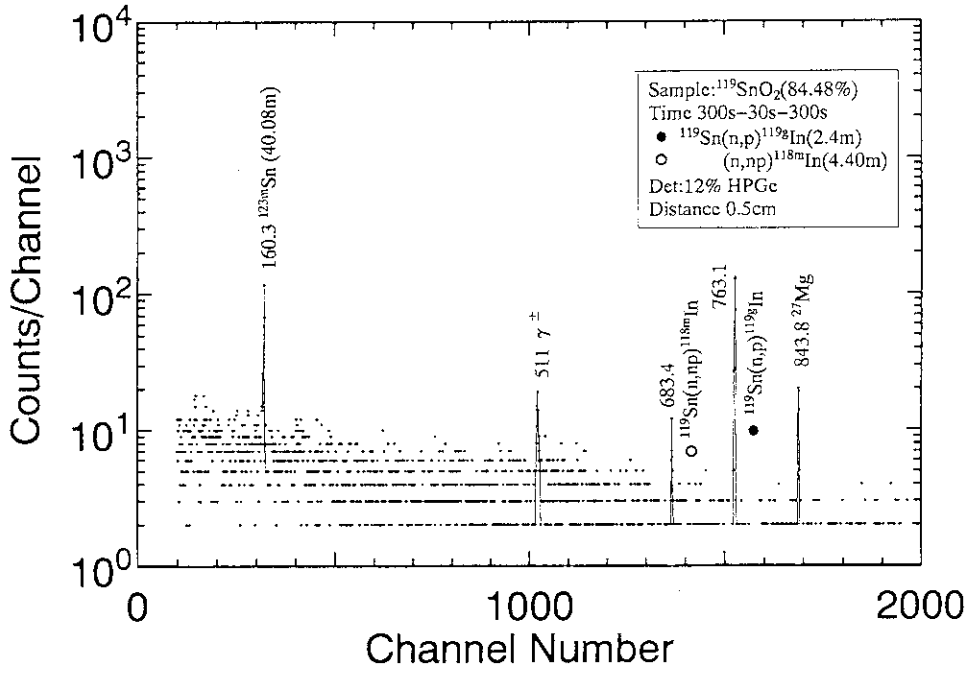

Fig. A.1.19

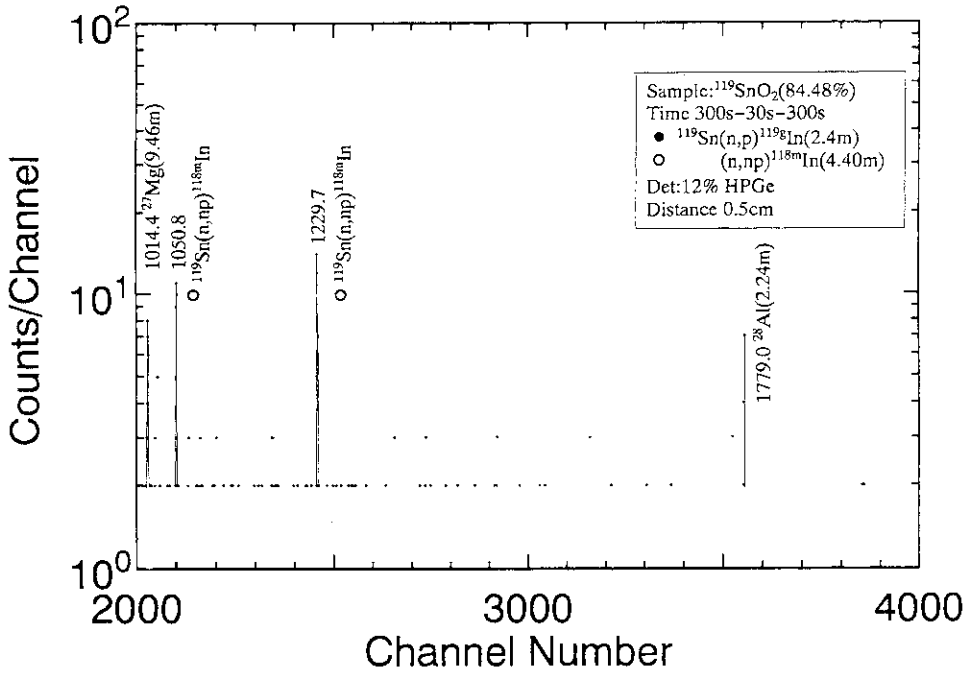

Fig. A.1.20

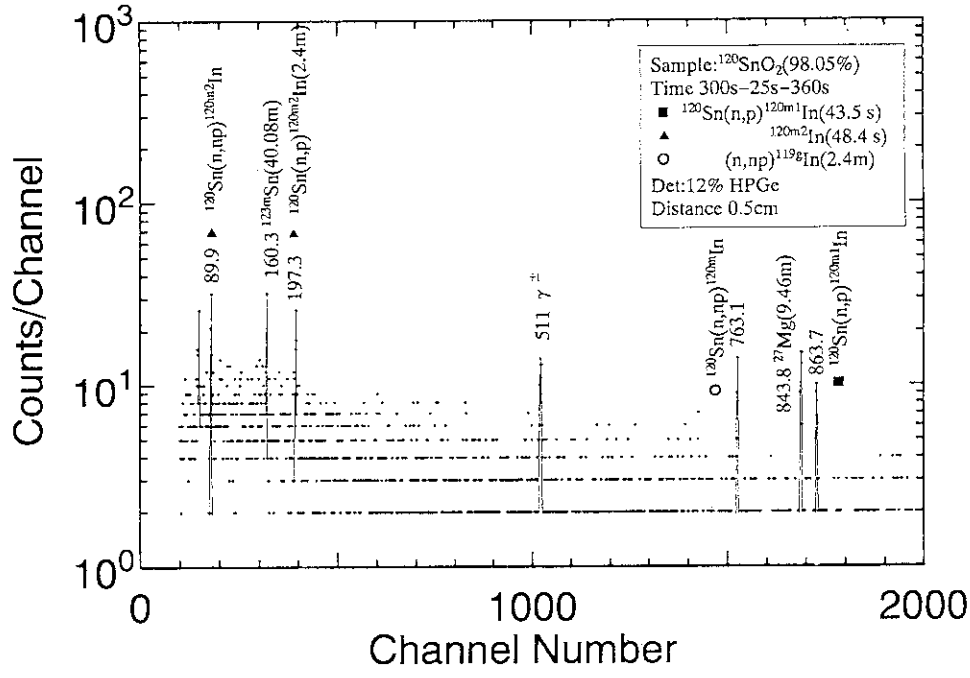

Fig. A.1.21

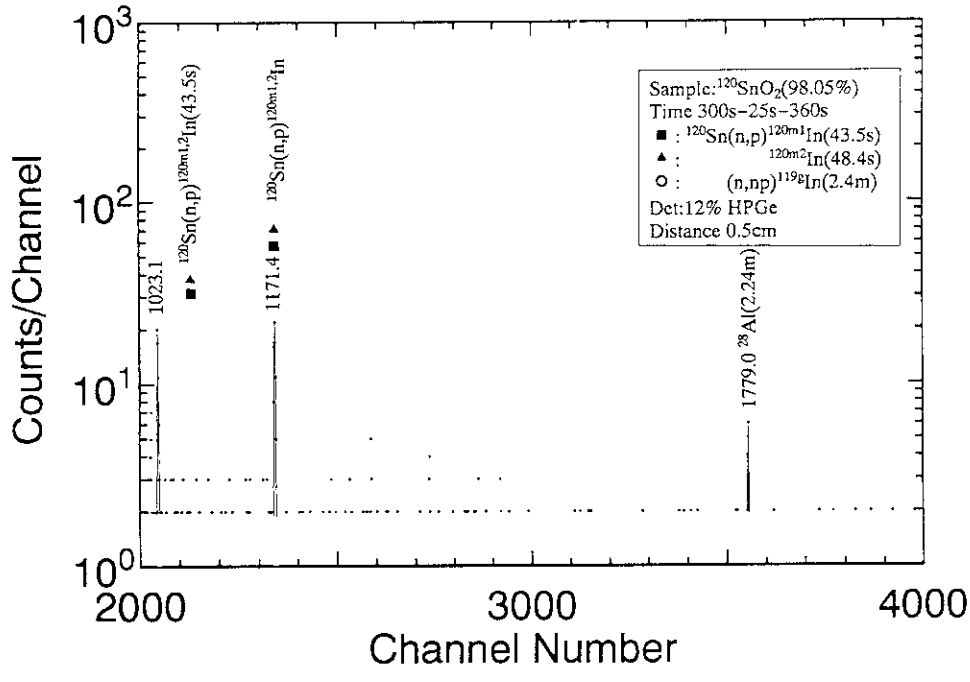

Fig. A.1.22